# Serine-404 Phosphorylation and the R406W Modification in Tau Stabilize the *cis*-Proline Amide Bond, via Phosphoserine-Proline C−H/O and Proline-Aromatic C−H/□ Interactions

Himal K. Ganguly, Michael B. Elbaum, and Neal J. Zondlo\*

Department of Chemistry and Biochemistry

University of Delaware

Newark, DE 19716

**United States** 

\* To whom correspondence should be addressed. email: *zondlo@udel.edu*, phone: +1-302-831-0197.

# **Abstract**

Tau misfolding, oligomerization, and aggregation are central to the pathology of Alzheimer's disease (AD), chronic traumatic encephalopathy (CTE), frontotemporal dementia, and other tauopathies. Increased phosphorylation of tau is associated with conformational changes that are not fully understood. Moreover, tau oligomerization and aggregation are associated with proline cis-trans isomerism, with the phosphorylation-dependent prolyl isomerase Pin1 reducing tau hyperphosphorylation and aggregation. The FTDP-17 tau mutation R406W is frequently used in animal models of Alzheimer's disease, due to earlier onset of the AD phenotype. Despite its extensive application, the mechanisms by which tau-R406W leads to enhanced aggregation and neurotoxicity are poorly understood. Peptides derived from the tau Cterminal domain were examined by NMR spectroscopy as a function of residue 406 identity (Arg versus Trp) and Ser404 phosphorylation state. The R406W modification led to an increased population of Pro405 cis amide bond, which is stabilized by cis-proline-aromatic C-H/ interactions. Ser404 phosphorylation also resulted in an increase in cis amide bond, via a proposed C-H/O interaction between the Pro H[] and the phosphate that stabilizes the cis conformation. An analogous C-H/O interaction was observed in Glu-cis-Pro sequences in the PDB, and is proposed to be the basis of the increased propensity for cis amide bonds in Glu-Pro sequences. The higher activation barriers for proline *cis-trans* isomerization observed at pSer-Pro and pThr-Pro sequences are proposed to be due to both (a) an intraresidue phosphate-amide bond that stabilizes the *trans*-proline conformation and (b) the *cis*-stabilizing proline-phosphate C-H/O interaction identified herein. The combination of both pSer404 and R406W resulted in a further increase in the population of cis amide bond. In contrast to expectations, the R406W modification led to increased dephosphorylation of either pSer404 or pSer409 by PP2A, and had no effect on phosphorylation of Ser404 by cdk5, suggesting that R406W does not inherently increase Ser404 phosphorylation via changes in the actions of these enzymes. Modestly increased phosphorylation of Ser404 was observed by GSK-3 in tau R406W. Collectively, these data suggest a potential role for conformational change to a cis amide bond at Pro405, via Ser404 phosphorylation and/or R406W modification, as a possible mechanism involved in protein misfolding in AD, CTE, and FTDP-17. Alternatively, both Ser404 phosphorylation and the R406W modification lead to increased order, including induced turn formation, in both the trans-proline and cis-proline conformations.

# Introduction

Misfolding and aggregation of the protein tau are central to the pathology of a range of neurodegenerative disorders, including Alzheimer's disease (AD), chronic traumatic encephalopathy (CTE), frontotemporal dementia and parkinsonism linked to chromosome 17 (FTDP-17), Pick's disease, and others, collectively termed tauopathies.<sup>1-8</sup> Tau is an intrinsically disordered protein (IDP) whose function is regulated by phosphorylation and other post-translational modifications, and which is important in normal physiological functions including axonal transport.<sup>9-11</sup> Tau is hyperphosphorylated in numerous tauopathies, with phosphorylation at a series of defined sites characteristic of the diseased state.<sup>12-16</sup>

Tau binds microtubules via its tubulin-binding domain (TBD), which contains four imperfect repeats of 31-32 amino acids (Figure 1). The hydrophobic TBD forms the core of disease-associated tau aggregates, which differs in structure in distinct disease-related neurofibrillary tangles.<sup>17-20</sup> However, most major disease-associated phosphorylation sites are located in the tau proline-rich domain (PRD) and the C-terminal domain (CTD), both of which lack well-defined structure even in aggregates.<sup>21-24</sup> For example, imaging of CTE typically employs antibodies against tau phosphorylated at phosphoserine (pS, pSer) and phosphothreonine (pT, pThr) residues in the proline-rich domain, (e.g. AT8, pS199/pS202/pT205).<sup>25,26</sup> A potential basis for the effects of phosphorylation in the PRD and CTD in inducing protein aggregation was provided by FRET experiments demonstrating that tau adopts a dynamic global hairpin structure, in which short hydrophobic segments within the N-terminal domain, proline-rich domain, and C-terminal domain fold against the hydrophobic TBD, reducing its solvent-exposed hydrophobic surface area.<sup>27,30</sup> Thus, these regions outside the TBD function to protect the TBD from aggregation by dynamically reducing the ability of the

hydrophobic sequences to self-associate and aggregate. The specific role of phosphorylation could be to provide electrostatic repulsion that opens the global hairpin, with pseudophosphorylation of the PRD or C-terminal domain inducing changes in rates of fibrillization and compactness of the global hairpin of tau. Turthermore, phosphorylation of tau can have specific structural effects, where phosphorylation in sequences derived from the tau PRD results in large local disorder-to-order transitions, including adoption of polyproline II helix and compact values of  $\phi$  at phosphorylated residues. 22,23,38-44

In addition to these effects, tau aggregation is regulated by the phosphorylationdependent proline isomerase Pin1, as well as by other prolyl isomerases. 45-51 Pin1 recognizes and lowers the activation barrier for proline cis-trans isomerism at phosphoserine-proline and phosphothreonine-proline sites.<sup>52-55</sup> Pin1 overexpression is associated with reduced tau aggregation and neurodegeneration in mouse models of AD, whereas Pin1 is depleted in human brains with AD. 46,56 Moreover, conformation-specific antibodies against pSer/pThr-cis-Pro and pSer/pThr-trans-Pro structures clearly indicate a role of proline cis-trans isomerism in protein misfolding.<sup>57,58</sup> In particular, most phosphatases<sup>47,59,60</sup> only act at pSer/pThr-trans-Pro amide bonds, and thus the presence of a cis amide bond will inherently increase the phosphate occupancy in most cases. In addition, proline *cis-trans* isomerism induces a substantial change in local structure, and can induce global changes in protein structure and function. <sup>61,62</sup> Furthermore, phosphorylation inherently increases the activation barrier for isomerization at a pSer/pThr-Pro amide bond, via mechanisms that are poorly understood. 45,63 In total, these observations suggest that protein misfolding and aggregation in tau could centrally involve proline cis-trans isomerization, either through direct changes in protein structure or through the more indirect mechanism of increasing phosphorylation site occupancy. However, a more detailed molecular explanation behind these potential mechanisms remains elusive.

In view of the broad complications of working with tau, including the inability to easily generate defined phosphorylation patterns in tau, rodent models have played a central role in associating tau misfolding, neurodegeneration, and behavioral effects. Tau is inherently a highly soluble protein. However, certain mutations in tau have been observed to lead to early-onset tauopathies in humans. Connecting human disease to molecular mechanisms, rodents with these tau mutations exhibit early onset of neurodegeneration and AD-like pathology. The substantial reduction in age of onset has led to tau-mutant mice and rats being widely employed, often in combination with AD-pathology-inducing mutations, greatly reducing the time required for animal experiments.

Mutations in the tau TBD (G272V, P301L, V337M) can promote ☐-sheet structure (G272V, P301L) and/or increase hydrophobicity (all three mutations) within the aggregation-prone region of tau.<sup>73-76</sup> However, a widely used tau disease-associated variant, the R406W mutation observed in human familial FTDP-17, occurs within the tau C-terminal domain.<sup>67</sup> Increased hydrophobicity at this position would not be expected to directly contribute to self-assembly of the TBD repeats, as it is outside of the self-assembling TBD region. Moreover, the R406W mutation could even potentially lead to reduced aggregation if it increases association of the CTD with the TBD, in a manner consistent with stabilizing the global hairpin. However, within aggregated protein models, in animal studies, and in humans, the tau R406W mutation is associated with increased levels of tau hyperphosphorylation and increased tau aggregation and disease pathology.<sup>69,70,73,77-82</sup> The identification of the mechanism(s) by which the R406W

mutation leads to increased tau aggregation and hyperphosphorylation could lead to fundamental insights into tau protein misfolding and the molecular mechanisms of human tauopathies.

#### **Results**

We sought to test a series of potential mechanisms by which the R406W mutation could lead to chemical and structural changes in tau that could result in increased tau aggregation. The mechanisms considered include the following:

- (1) The increased hydrophobicity of tryptophan versus arginine. Arginine (R) is polar, while tryptophan (W) is the most hydrophobic of the canonical amino acids (Figure 1c).
- (2) Increased Ser404 phosphorylation due to changes in substrate recognition by kinases. Ser404 phosphorylation is a major phosphoepitope in tau, where it is present as a pSer-Pro site. An increase in Ser404 phosphorylation is observed in disease using the PHF-1 antibody specific to this site and to pSer396.<sup>83,84</sup> In addition, Ser404 pseudophosphorylation leads to changes in rates of aggregation and changes in the global hairpin structure.<sup>31,32,34-36,85</sup> Ser404 phosphorylation could potentially be increased through changes in kinase recognition via the protein kinases cdk5 or GSK-3[], both of which phosphorylate this site.<sup>86-91</sup> The amino acid that is 2 residues after a phosphorylation site (P+2 position; here, residue 406) is often a major determinant of protein kinase specificity, and increased action of the kinase on this site would lead to higher overall phosphorylation stoichiometry.
- (3) Increased population of cis amide bond at pSer404-Pro405 due to phosphorylation at Ser404.<sup>45</sup>
- (4) Increased population of *cis* amide bond due to an aromatic residue following proline, via a *cis*-proline-aromatic interaction (Figure 1d). 92-99 Additionally, local order can be induced

inherently in proline-aromatic sequences, in both the *trans*-proline and *cis*-proline conformations.<sup>99</sup>

(5) Decreased rate of enzymatic dephosphorylation by phosphatases. Reduced phosphatase activity could occur through a direct sequence effect (substrate specificity) in reducing the rate of dephosphorylation.<sup>51,100-103</sup> Alternatively, either or both of mechanisms (3) or (4), by increasing the population of *cis* amide bond, could increase the stoichiometry of phosphorylation at pSer404 by decreasing the rate of dephosphorylation via reducing the population of species with a *trans* amide bond that is required by the phosphatase.<sup>47</sup> Notably, pSer404 is a priming site for phosphorylation of Ser400 and Ser396 by GSK-3[].<sup>104</sup> Increased phosphorylation at pSer404 would thus be expected to inherently increase the stoichiometry of phosphorylation at both Ser396 and Ser400.

Analysis of the effects of Ser404 phosphorylation and R406W modification on the Pro405 cis-trans isomerism equilibrium. To address these potential mechanisms, we examined tauderived peptides, in order to obtain molecular-level understanding via NMR spectroscopy. The peptides  $tau_{395.411}$  and  $tau_{395.411}$ –R406W were synthesized both in non-phosphorylated forms and phosphorylated at Ser404 ( $tau_{395.411}$ –pS404 and  $tau_{395.411}$ –pS404—R406W) (Figure 1b). These peptides were examined by NMR spectroscopy, in order to identify potential effects of Ser404 phosphorylation and the R406W modification on proline-405 cis-trans isomerism (Figure 2, Table 1). Consistent with hypotheses 3 and 4, phosphorylation of Ser404 was observed to significantly increase the population of Pro405 cis amide bond ( $K_{trans/cis}$  = [population with trans amide bond]/[population with cis amide bond]; a smaller  $K_{trans/cis}$  indicates a higher population of cis amide bond). In addition, the R406W modification also increased the population of cis amide

bond, in both the non-phosphorylated and phosphorylated peptides. Notably, the peptide with the dianionic form of phosphoserine, which is the major form at physiological pH (typical p $K_a$  5.5–6.0), exhibited the highest population of cis amide bond.

In order to obtain deeper understanding of the nature of the interactions that lead to increased *cis* amide bond at this site, we examined a series of tetrapeptides Ac-T(S/pS)P(R/W)-NH<sub>2</sub> derived from *tau*<sub>403-406</sub>. (Figure 3, Table 2). These tetrapeptides allow the resolution and unambiguous assignment of the NMR resonances associated with the *trans* and *cis* amide bonds. We observed similar effects in the tetrapeptides as in the larger tau peptides, with both phosphorylation and the R406W modification increasing the population of *cis* amide bond, with the peptide containing *both* pS404 *and* W406 exhibiting 24% *cis* amide bond at pH 7.2, compared to only 11% *cis* amide bond for the peptide with Ser404 and R406. Again, the population of *cis* amide bond was highest at physiological pH, where pSer exists predominantly in the dianionic ionization state.

The effects of R406W alone on increasing the population of cis-Pro were relatively small in the peptide with non-phosphorylated Ser, in contrast to prior data in model peptides.  $^{92,95,97,99,105}$  However, prior results on peptides with X-Pro-aromatic sequences indicated that [non-phosphorylated] Ser relatively disfavored proline-aromatic interactions that stabilize cis-Pro. Interestingly, the effects of Ser404 phosphorylation and R406W modification on the amount of observed cis amide bond were more than additive, with a greater effect on  $\Box\Box G_{trans/cis}$  with both changes present than the sum of the effects of the individual changes. These data suggested the possibility that phosphorylation and the R406W modification might be synergistic in promoting cis amide bond.

Further analysis of the NMR data (Table 3; Tables S10-S13) indicated substantial ordering upon each of phosphorylation and the R406W modification. Phosphorylation increased the amide chemical shift ( $\square$ ) dispersion in both peptide series, consistent with increased order upon phosphorylation, in both *trans*-Pro and *cis*-Pro. In addition, the peptide TpSPW exhibited  ${}^3J_{\square N}$  values consistent with substantial ordering in both the *trans* and *cis* conformations.  ${}^3J_{\square N}$  correlates with the  $\phi$  torsion angle; the further from the ~7 Hz value for a random coil, the greater the ordering. In TpSPW, a more extended conformation was observed at Thr (larger  ${}^3J_{\square N}$ ; *cis* 8.9 Hz) and a more compact conformation was observed at pSer (smaller  ${}^3J_{\square N}$ ; *cis* 5.5 Hz), with larger effects (= more order) in the *cis*-proline conformation.

In addition, temperature-dependent NMR data (between 4 °C and 37 °C) on the phosphorylated peptides as a function of pH revealed that the  $K_{\text{trans/cis}}$  was largely temperature-independent (Table S12), suggesting that these observations apply to physiological conditions. Moreover, these data for *cis*-Pro also indicated a substantial decrease in the magnitude of the amide chemical shift temperature coefficient ( $|\Box VK|$ ) at Thr and pSer, and a significant increase for Trp, in TpSPW compared to TpSPR (Table S13). Collectively, the chemical shift and  $^3J_{\Box N}$  data are consistent with a substantial increase in order for TpSPW due to both phosphorylation and the R406W modification.

In general, Pro-Trp sequences exhibit significant order, in both the *trans*-Pro and *cis*-Pro amide conformations, due to favorable C–H/ $\square$  interactions of the aromatic ring with the proline ring (Pro-aromatic interactions) and/or with the H $\square$  and/or the side chain hydrogens of the pre-proline residue (H $\square$ -Pro-Trp interactions). In *cis*-Pro-aromatic sequences, the *cis* amide conformation can be stabilized via the interaction of the aromatic ring with H $\square$  of the residue

before proline (here, Ser H $\square$ ) or via the interaction of the aromatic ring with H $\square$ , H $\square$ , and/or H $\square$ of the proline ring (Figure 1d). 93-98,107 Similar interactions are observed for trans-Pro, with the additional possibility for Trp to interact simultaneously at both the P-1 residue and at Pro. These interactions are stronger for Trp than for other aromatic amino acids, and lead to a strong propensity for turns at Pro-Trp sequences. While interaction at the Pro ring is more entropically favorable, the interactions at the pre-Pro residue (here, Ser or pSer) are stronger, and those interactions specifically promote conformations that are typically disfavored. Examining chemical shifts in the aliphatic region of the spectra (Figures 3c-3d, Table 3, Table S10), for the peptides with Trp, the Ser or pSer H $\square$  was shifted 0.39 ppm upfield in the *cis* conformation, compared to a 0.13-0.20 ppm upfield shift in the cis conformation for the peptide with Arg. The Pro H $\square$  were similarly shifted significantly upfield in the *cis* conformations compared to the trans conformations in peptides with Trp, but not in peptides with Arg. The Ser or pSer H□ are also upfield shifted in peptides with Trp compared to equivalent peptides with Arg, consistent with H\[\int\_\text{-trans-Pro-Trp interactions.}\] These NMR data are consistent with Trp406 interacting with these hydrogens to relatively stabilize the cis-Pro conformation, and to stabilize distinct conformations and induce order in both proline amide conformations, in peptides with the R406W modification.

In peptides containing pSer, a downfield change in the Pro H $\square$  chemical shift was observed in the *cis* amide conformation, compared to the equivalent peptides with Ser (Figure S5, Tables S3-S8). In addition, the pSer amide hydrogens (H $^N$ ) were shifted downfield, compared to the Ser amides of the equivalent peptides, as we had previously observed both in tau-derived peptides and in model peptides.<sup>38,39,108-111</sup> In both of these cases, the chemical shift changes (downfield pSer H $^N$  for *trans* amides, downfield Pro H $\square$  for *cis* amides) were substantially

greater in the dianionic form of pSer. We previously identified that the downfield shift in  $H^N$  of pSer in *trans* amides was due to an intraresidue phosphate-amide hydrogen bond that stabilizes a compact value of  $\phi$  ( $\Box$ -helix or polyproline II helix (PPII)). The downfield change in Pro  $H\Box$  chemical shift suggested the possibility that an interaction between the phosphate and the Pro  $H\Box$  could stabilize the *cis* amide conformation.

At pSer-Pro and pThr-Pro sequences, phosphorylation increases the activation barrier for proline *cis-trans* isomerization, through mechanisms that are not well understood. These data suggested the possibility that phosphorylation could lower the energy of both the *trans* amide conformation (via an intraresidue phosphate-amide hydrogen bond) and the *cis* amide conformation (through a putative Pro-C-H[]/phosphate C-H/O interaction), which would result in a higher activation barrier if these interactions are not present in the transition state. These potential stabilizing interactions will be further explored below.

Effects of the tau R406W modification on tau phosphorylation by cdk5 and GSK-3β. The identities of the amino acids local to the phosphorylation site are central determinants of protein kinase substrate specificity. Residue 406 is two amino acids after the Ser404 phosphorylation site (P+2 position). The identity of the amino acid at the P+2 position can have substantial effects on substrate recognition and the rate of enzymatic phosphorylation. The differences between the cationic charged, polar residue Arg and the neutral, hydrophobic, aromatic residue Trp at the P+2 position thus could potentially dramatically affect rates of phosphorylation by cognate kinases.

Ser404 in tau is phosphorylated by the proline-directed kinase cdk5.  $^{87,89,90,115,116}$  In order to assess whether the R406W modification significantly modifies phosphorylation by cdk5, we examined phosphorylation of  $tau_{395,411}$  peptides with Arg or with Trp at residue 406 (Figure 4).

These peptides were allowed to incubate with cdk5/p35 and analyzed by HPLC to quantify the extent of phosphorylation as a function of reaction time (Figure 4a). The data indicated that the rates of phosphorylation of both the native sequence and the R406W variant by cdk5/p35 were similar (within experimental error).

Ser404 is also phosphorylated by GSK-3 a protein kinase whose recognition sequence includes a priming phosphorylation site that is 4 or 5 residues C-terminal (P+4 or P+5 position) to the residue to be phosphorylated. Ser409 is a well-documented site of tau phosphorylation. Phosphorylation at Ser409 thus generates an appropriate priming site for phosphorylation at Ser404 by GSK-3 Therefore,  $tau_{395-411}$  peptides were synthesized with Ser409 phosphorylated, and assessed for phosphorylation at Ser404 by GSK-3, as a function of the identity of residue 406. The data (Figure 4b) revealed only a very small difference in the rates of phosphorylation between the peptides, with the R406W variant showing modestly faster phosphorylation. In the context of quantified phosphorylation rates by protein kinases of substrates as a function of amino acid identity, the rate differences observed for phosphorylation by cdk5/p35 and by GSK-3 upon R406W substitution are minimal. While protein-protein interactions can substantially impact protein kinase recognition, overall these data indicate that the R406W modification is unlikely to substantially increase protein phosphorylation by the well-studied tau kinases cdk5 or GSK-3.

Effects of R406W modification on tau dephosphorylation by protein phosphatase 2A (PP2A). PP2A is a major intracellular protein phosphatase, and has been studied extensively for dephosphorylation of hyperphosphorylated tau. <sup>47,51,102,103,118,119</sup> In tau, residue 406 is proximal to the phosphorylation sites pS404 and pS409. The R406W modification thus could potentially cause an increase in phosphorylation levels at these sites via a reduction in phosphatase-mediated

dephosphorylation, due to the presence of Trp 2 or 3 residues from the site of dephosphorylation. In addition, like most protein phosphatases, PP2A is specific to dephosphorylation at *trans* amide bonds.<sup>59,60,120</sup> Thus, the increased presence of *cis* amide bonds in R406W tau could potentially further decrease the rate of dephosphorylation at pS404 due to the increased presence of *cis*-proline at Pro405.

tau<sub>395-411</sub> peptides, in both Arg406 and Trp406 variants, with phosphorylation at either Ser404 or Ser409, were analyzed for dephosphorylation by PP2A as a function of time, and the relative rates were quantified (Figure 5). PP2A did not detectably dephosphorylate  $tau_{395-411}$  with phosphorylation at Ser404 and Arg at residue 406. In contrast, PP2A readily dephosphorylated pSer404 when Trp was present at residue 406. Thus, the R406W modification surprisingly resulted in at least a 2000-fold increase in the rate of dephosphorylation at pSer404. Dephosphorylation at pSer409 was also increased in the tau R406W variant, to a significant, though less dramatic, 2.5-fold effect. These data indicate that the R406W modification does not increase the phosphorylation occupancy at Ser404 or pSer409 as a result of decreased PP2A activity in the R406W variant. Indeed, pSer404 and pSer409 are more prone to dephosphorylation by PP2A with Trp at residue 406. Interestingly, these results are consistent with some (but not all) data that indicated lower levels of Ser404 phosphorylation in soluble R406W-tau, 78-80 in contrast to the higher levels of phosphorylation in aggregated R406W-tau in vivo. 69,70,80-82 Collectively, the data on the effects of the R406W modification on protein kinase and protein phosphatase activities indicate that Trp406 is unlikely to increase phosphorylation site occupancy at Ser404 or Ser409 via effects in increasing kinase activity or in decreasing phosphatase activity via the enzymes studied.

Bioinformatics analysis of Glu-Pro structures in the PDB. In tau<sub>395-411</sub> and tau<sub>403-406</sub> peptides, phosphorylation led to an increased population of *cis* amide bond, both with the native Arg at residue 406 and with the R406W modification. In both cases, the increase in population of *cis* amide bonds was greatest with pSer in the dianionic ionization state. Ser and Thr phosphorylation have previously been shown to increase the activation barrier of proline *cis*-trans isomerization at pSer-Pro and pThr-Pro sites.<sup>45</sup> In addition, in *some* cases, but certainly not in all cases, phosphorylation can increase the population of *cis*-Pro amide bond. However, the basis for these observations is poorly understood. There is no example in the PDB of an isolated pSer-*cis*-Pro (i.e. not part of a protein complex where one protein specifically recognizes *cis*-Pro). Therefore, in order to understand the molecular basis for these observations, we examined structures of the phosphomimetic amino acid Glu in Glu-Pro structures in the PDB, as a function of proline *cis* versus *trans* amide conformation.

Notably, Glu-Pro sequences exhibited a greater likelihood of adopting a *cis*-Pro amide bond than the average frequency across all amino acids (Glu-Pro 6.9%, all X-Pro 5.2%), consistent with prior analyses of the PDB. <sup>121-123</sup> Among encoded amino acids, Glu is most similar in size to pSer, with both pSer and Glu having the terminal oxygens 4 bonds away from C. Therefore, we more carefully examined these structures, in order to identify a potential basis for Glu and pSer to stabilize the *cis*-proline conformation.

Analysis of the carboxylate oxygen•••Pro  $\mathbb{C}[]$  distances revealed a striking difference between interactions of the side chain with the backbone in *trans*-Pro versus *cis*-Pro structures (Figure 6). With a *trans*-Pro conformation, the Glu carboxylate was rarely (5%) in close proximity ( $\leq 4.25 \text{ Å O}$ •••C distance) to the Pro  $\mathbb{C}[]$ . In contrast, with a *cis*-Pro conformation, the Glu carboxylate was near the Pro  $\mathbb{C}[]$  in nearly half (48%) of all structures.

Closer investigation of the Glu-cis-Pro structures, with hydrogens added computationally, revealed that Glu carboxylates here were engaging in a particularly close C–H/O interaction with the Pro C $\Box$ -H $\Box$  bond. C–H/O interactions occur predominantly at polarized C–H bonds with a significant  $\Box$ <sup>†</sup> on the hydrogen. <sup>124-134</sup> The C $\Box$ -H $\Box$  bond of an  $\Box$ -amino acid is adjacent to both the electron-withdrawing carbonyl and the amide nitrogen, and thus H $\Box$  has substantially greater  $\Box$ <sup>†</sup> than other aliphatic side chain hydrogens. This reduced electron density at H $\Box$  is identified via its more downfield chemical shift compared to other aliphatic protein hydrogens. These properties of protein  $\Box$ -hydrogens make them particularly favorable for both C–H/O interactions (here) and C–H/ $\Box$  interactions (with aromatic amino acids).

The strength of these Pro C-H[]-Glu carboxylate C-H/O interactions can be assessed in part by the H-O distances (Figure 6c), which in the examples analyzed were substantially below the 2.72 Å sum of the van der Waals radii of O and H. These close distances suggest that these interactions are quite energetically favorable. Moreover, C-H/O interaction strength depends on the charge on oxygen: prior computational investigations have indicated that monoanionic oxygen electron sources (such as Glu) have stronger C-H/O interactions than neutral oxygen electron donors, and that dianionic oxygen electron sources (such as in dianionic pSer) have stronger C-H/O interactions than monoanionic oxygen electron sources. Thus, the bioinformatics data strongly suggest that Glu stabilizes a *cis*-Pro amide conformation in Glu-Pro sequences via a C-H/O interaction between the Glu carboxylate and the Pro C-H[]. These data further suggest that dianionic pSer can engage in similar C-H/O interactions that stabilize a *cis*-proline amide bond, and that these interactions should be even stronger in dianionic pSer than in Glu.

Computational investigation of Glu-cis-Pro and pSer-cis-Pro C-H/O interactions. In order to obtain further insights into the C-H/O interactions that are proposed herein to stabilize the cis-Pro conformation, a series of computational investigations was initiated (Figure 7). 136-140 Constructs were generated based on a series of protein structures (Figure 6c, Figure 8) with a Glu-cis-Pro conformation, representing distinct protein main-chain conformations. These protein chains were initially reduced to 2-residue protein models and analyzed computationally. In addition, these models were further reduced to minimal structures of complexes between an acetate anion (Glu-derived carboxylate) and a minimal For-Pro-NH<sub>2</sub> peptide. This AcO-•For-Pro-NH<sub>2</sub> complex approximates the electrostatics of the native Glu-cis-Pro structure, and maintains the protein geometry, while representing the interaction as a bimolecular complex. This approach allowed the analysis of C–H/O interaction energetics in a model tractable with the MP2 level of theory, and with a sufficiently large basis set (aug-cc-pVTZ) to minimize artefacts observed when smaller basis sets are employed. These analyses were supplemented by calculations using natural bond orbital (NBO) analysis, 141,142 which allows the analysis of molecular orbital contributions to interaction energies.

The calculations indicated that these Glu-*cis*-Pro C–H/O interactions have a substantial (1.5–2.4 kcal mol<sup>-1</sup>) interaction energy in implicit water. These interaction energies are not free energies, as they do not address competitive solvation nor entropic effects. Nevertheless, they indicate that Glu-*cis*-Pro C–H/O interactions can provide an energetic basis for stabilizing the *cis*-proline amide conformation in water. The C–H/O interaction includes an electrostatic component, between the negatively charged carboxylate and the []<sup>+</sup> on Pro H[]. The role of electrostatics is clearly identified by the far larger interaction energies in the gas phase (7–17 kcal mol<sup>-1</sup>) compared to in implicit water. In addition to electrostatics, NBO analysis indicated

that the interaction strength is significantly dependent on molecular orbital interactions (stereoelectronic effects), via orbital overlap between Glu carboxylate lone pairs (n) and the [\* molecular orbital of the Pro C[-H[] bond (as an n[] [\* interaction), which results in electron delocalization between the carboxylate and the proline ring.[134

In order to understand how pSer stabilizes the *cis* amide conformation at Pro405 in tau, a computational model of a pSer-*cis*-Pro structure was developed, using the Glu-*cis*-Pro structures identified via bioinformatics to generate initial models. These models were subjected to geometry optimization using DFT methods. The resultant model of a minimal Ac-pSer-*cis*-Pro-NHMe peptide exhibited a close C–H/O interaction (2.24 Å H

—O distance) between the pSer phosphate O and the Pro H

[Figure 7]. The resultant geometry was similar to that observed in Glu-*cis*-Pro interactions in the PDB.

This computationally optimized structure was then further analyzed as a minimal dianionic methylphosphate MeOPO<sub>3</sub><sup>2</sup>•For-Gly-NH<sub>2</sub> complex, for comparison to the minimalist AcO•For-Gly-NH<sub>2</sub> complexes described above. As was the case for Glu-*cis*-Pro C–H/O interactions, these calculations indicated a significant interaction energy in implicit water (3.0 kcal mol<sup>-1</sup>) and in the gas phase (26 kcal mol<sup>-1</sup>), consistent with the Pro•pSer C–H/O interaction being quite favorable and having a partial electrostatic basis, though the electrostatic interaction energy should be relatively modest in water (Figure 7, Tables S19 and S20). <sup>134</sup> In addition, NBO analysis indicated a large molecular orbital overlap/electron delocalization contribution (as a phosphate O[] H[]—C[] n[] []\* interaction) to stabilization of the pSer-*cis*-Pro conformation. Collectively, the calculations strongly suggest that Glu-*cis*-Pro interactions are stabilized by a C–H/O interaction between the Glu carboxylate and the Pro C–H[]. Moreover, the computational models suggest that pSer stabilizes a *cis*-proline amide bond through an analogous pSer-*cis*-Pro

C–H/O interaction. This C–H/O interaction is stronger than the analogous Glu-*cis*-Pro interaction due to the dianionic ionization state of pSer, which makes the interacting oxygen a better electron donor. These data suggest a basis for prior results<sup>45</sup> showing that Ser/Thr phosphorylation increases the activation barrier for proline *cis-trans* isomerization: pSer and pThr can stabilize the *cis* amide conformation via a phosphate-Pro C–H/O interaction, and can stabilize the *trans* amide conformation via an intraresidue phosphate-amide hydrogen bond. Collectively these interactions stabilize both the *trans* and *cis* amide conformations, without impacting the energy of the *cis-trans* isomerization transition state, thus resulting in a larger overall activation barrier and reduced rate of proline *cis-trans* isomerization at pSer/pThr-Pro sequences.

Bioinformatics investigations also identified a structure (pdb 1obb<sup>143</sup>) with a Glu-*cis*-Pro-Trp sequence (Figure 8). The key interaction elements of this structure are proposed to be analogous to those of the pSer-*cis*-Pro-Trp structure in tau phosphorylated at Ser404 and with the R406W modification. In this structure, the effects of both a Glu-*cis*-Pro conformation stabilized by a C–H/O interaction and a *cis*-Pro-Trp C–H/\(\subseteq\) interaction combine to promote a *cis* amide bond conformation, as was observed in *tau*<sub>395-411</sub>–R406W or *tau*<sub>403-406</sub>–R406W peptides phosphorylated at Ser404. Computational investigations on minimal structures derived from this protein indicated that both interactions had substantial energetic contributions, with each stabilizing the *cis*-Pro conformation via both electrostatic and electron delocalization (molecular orbital-based/stereoelectronic) contributions. In addition, calculations indicated that this combination of interactions could promote an \(\subseteq\)-turn conformation, <sup>144,145</sup> as is present in 1obb, or a type VI \(\subseteq\)-turn conformation, <sup>146,147</sup> which is inherently promoted by *cis*-Pro-aromatic

interactions  $^{93-95,97,99,107,148}$  and is present in Glu-cis-Pro-aromatic capping motifs at the N-terminus of  $\square$ -helices.  $^{149}$ 

We have previously identified that Pro-Trp sequences can stabilize both turn geometries and structures in disfavored regions of the Ramachandran plot, via C−H/□ interactions and the hydrophobic effect, in both *cis*-Pro and *trans*-Pro.<sup>99</sup> Therefore, we computationally investigated potential structures involving noncovalent interactions of pSer and/or Trp that might promote turns and/or local order in tau, as a function of Ser404 phosphorylation and/or the R406W mutation. These geometry-optimized structures (Figure 9) build on our prior investigations of structure stabilization in Pro-Trp sequences, adding in observed pSer conformations with full geometry optimization. <sup>99,146,150</sup>

The computational results indicate that the R406W modification can specifically stabilize  $\Box$ -turn conformations, in both *trans*-Pro and *cis*-Pro, via C–H/ $\Box$  interactions at C–H bonds in pSer and/or at Pro. In these models, these C•••H aromatic contacts are below the 2.90 Å sum of the van der Waals radii of H and C, suggesting particularly favorable interactions. In addition to promoting  $\Box$ -turn geometries, these interactions are specifically capable of promoting disfavored regions of protein conformational space, including the  $\Box$ L conformation ( $\phi$ , $\psi$  on the right side of the Ramachandran plot), *cis*-proline ( $\omega \sim 0^{\circ}$ ), the sterically disfavored  $g^{+}\chi_{1}$  rotamer, and/or the  $\zeta$  conformation ( $\phi$ , $\psi \sim -130^{\circ}$ , +70°). Furthermore, the calculations indicate that pSer can, in some cases, provide additional stabilization to these observed conformations. For *trans*-Pro, hydrogen bonding of the pSer phosphate can specifically promote a type I  $\Box$ -turn centered on pSer–Pro by electronically strengthening the hydrogen bond of the  $\Box$ -turn. Additional phosphate interactions with the indole ring were also observed in some of these structures, although the importance of these phosphate-indole hydrogen bonds in water is less clear, especially because those

interactions are longer range and would have a greater entropic cost. For *cis*-Pro, pSer was observed in a close C–H/O interaction with the Pro C–H□ in multiple turn/aromatic interaction geometries. The closest C–H/O interactions here approached the distances of weaker hydrogen bonds, and were all well below 2.72 Å. These results suggest that C–H/□ interactions (for R406W tau) and C–H/O interactions (for pSer404) can function simultaneously to promote ordered turn conformations in the C-terminal domain of tau.

## Discussion

The R406W mutation in tau is associated with early-onset dementia and tauopathy in FTDP-17.<sup>67,80</sup> The tau R406W mutation is widely used in rodent models of Alzheimer's disease, introduced alone or in combination with other mutations, because of the significant reduction in the age of onset of AD-like symptoms and neuropathology.<sup>69,70,82</sup> However, despite its wide use, the mechanisms by which the R406W modification in tau can result in the dramatic effects observed *in vivo* remain poorly understood. Herein, we examined within peptides a series of potential mechanisms by which the effects of this sequence change could be realized. We considered inherent physical effects, effects on conformation, effects on enzymatic activity, and the interplay thereof.

Peptides derived from  $tau_{395.411}$  were examined by NMR spectroscopy as a function of phosphorylation state and of the identity of residue 406. The NMR spectra revealed that these peptides exist predominantly in a disordered conformation, with little amide chemical shift dispersion, as expected based on studies in the native non-phosphorylated tau protein. The tau C-terminal domain in particular is poorly characterized structurally, but exhibits no defining features or functions that suggest the adoption of regular secondary structure.

One key feature identified in  $tau_{395-411}$  was the presence of peptide with a cis-Pro amide bond. Notably, the extent of cis amide bond was significantly increased upon phosphorylation, which also led to local ordering at the pSer residue (Figure 2, Table 1). In addition, the R406W modification independently led to an increase in population of cis amide bond. The peptide that was both phosphorylated at Ser404 and had Trp at residue 406 exhibited the highest population of cis amide bond. These results in  $tau_{395-411}$  were confirmed in shorter  $tau_{403-406}$  peptides (Figure 3, Table 2), which allowed more detailed characterization of the independent and additive effects of Ser404 phosphorylation and R406W modification (discussed below).

Effects of the tau R406W modification on enzyme activity by cdk5, GSK-3 $\beta$ , and PP2A. The sequence specificities of protein kinases and protein phosphatases depend on factors including local sequence identity and protein-protein interactions. The modification at residue 406 in tau from Arg to Trp results in the change from a positively charged, polar side chain to a neutral, aromatic, and highly hydrophobic side chain. Arg residues have unique roles in increasing the sequence specificity of numerous protein kinases and phosphatases, and as such the R406W modification could dramatically change the reactivity of the tau protein toward enzymatic phosphorylation and/or dephosphorylation. For example, the protein kinases PKA, Akt, and Pim2 have a strong preference for Arg at the amino acid 3 residues prior (P–3 position) to the phosphorylation site, and a significant selection against Trp at these sites. H4.117 Thus, kinase substrate array data indicate 40-fold, 350-fold, and 300-fold reductions in phosphorylation when Arg is replaced by Trp at the P–3 position in a PKA, Akt, or Pim2 substrate, respectively. Notably, these data from Turk and coworkers strongly suggest that the R406W modification should greatly reduce phosphorylation at Ser409 by these and related kinases.

Hyperphosphorylation of tau, in particular at Ser404, which is observed using the PHF-1 antibody, is a hallmark of tau in AD.<sup>83</sup> Here, we examined how the R406W modification would impact phosphorylation at Ser404 by cdk5 and GSK-3, and dephosphorylation at pSer404 by PP2A. These kinases have been broadly implicated in the regulation of tau phosphorylation, specifically at Ser404 (in the case of GSK-3, when Ser409 is phosphorylated).<sup>86-89,103,118,153</sup> In *tau*<sub>395-411</sub> peptides, no substantial impact was observed for the R406W modification on the rate of phosphorylation by these kinases. The only change identified was a modest increase in phosphorylation in R406W by GSK-3. As such, a significant increase in tau phosphorylation due to increased activities of these enzymes on R406W tau seems unlikely to be a basis for the effects of this mutation.

Proline *cis-trans* isomerism is a slow step in protein folding and can result in large changes in the structure and function of proteins. These large structural effects mean that the *trans* and *cis* amide conformations are not recognized as equivalent at enzyme active sites. In particular, protein phosphatases at pSer-Pro sites exhibit specificity for either the *trans* or *cis* Pro amide conformation. The phosphatases previously demonstrated to dephosphorylate tau appear to be specific for the *trans*-Pro conformation. Thus, based on the increased population of *cis* amide bond when Ser404 is phosphorylated and/or with Trp at residue 406, one would expect, in R406W tau, that phosphatase activity might be reduced at pSer404 due to an increased population of pSer404-*cis*-Pro405 amide bond. In order to understand the sequence effects of the R406W modification on protein phosphatase activity, we examined the activity of PP2A at both pSer404 and pSer409. Surprisingly, the R406W modification significantly *increased* dephosphorylation at pSer404 and pSer409. Indeed, pSer404 was only significantly dephosphorylated by PP2A in the tau R406W variant. These data indicate that the R406W

modification should actually *decrease* the extent of tau phosphorylation at Ser404 and Ser409 due to the more rapid dephosphorylation of R406W tau by PP2A, as has been seen in some studies on soluble tau. R406W tau than in wild type tau, these data suggested the possibility that other factors in R406W tau could contribute to functional changes, which are inherently linked to structure.

Effects of the R406W modification on Pro405 cis-trans isomerism: structural effects in proline-aromatic sequences. In  $tau_{395-411}$  and  $tau_{403-406}$  peptides, both phosphorylation and the R406W modification were observed to increase the population of cis-Pro amide bond. In addition, in the cis amide conformations with the wild-type tau sequence, the Arg406 amide resonance shifted significantly downfield. These observations suggested the possibility that both changes could potentially promote cis amide bond and induce turn conformations. Notably, Thr is the most favorable residue at the i position of type VI  $\Box$ -turns (where Thr403 would be in a  $\Box$ -turn centered on pSer-cis-Pro).  $^{95,147}$ 

However, the mechanisms by which either phosphorylation at Ser404 or the R406W modification could lead to increased cis-Pro405 amide bond remain poorly understood, despite both sequence effects Pro amide conformation being described on previously. 45,92,94,95,97,98,107,148,158,159 A deeper understanding of the bases for these sequence effects to impact protein conformation and structure could have specific implications in understanding the possible mechanisms of tau misfolding. In addition, a detailed analysis could elucidate more general effects of phosphorylation at Ser/Thr-Pro sites and proline-aromatic sequences to impact protein structure.

Phosphorylation at Ser404 promotes a cis-proline conformation at Pro405 via a prolinephosphate C–H/O interaction. We observed that Ser404 phosphorylation significantly increases the population of cis amide bond at Pro405. This increased population of cis amide bond was observed both in peptides with native tau sequences, with Arg at residue 406, and in tau peptides with the R406W modification. Further analysis of the NMR data indicated three significant trends in the cis-Pro conformation: (1) the Pro H $\Box$  chemical shift exhibited a downfield change in the phosphorylated peptides; (2) backbone ordering was observed both as a result of phosphorylation and of the R406W modification, based on values of  ${}^3J_{\Box N}$  that deviated further from random coil values; and (3) the residue 406 (Arg or Trp) H $^N$  exhibited substantial downfield shifts in the cis amide bond as a result of phosphorylation, indicating specific ordering at the post-proline residue due to phosphorylation.

Notably, the very downfield  $\Box$  of the H<sup>N</sup> of Arg406 in the *cis*-Pro conformation of TpSPR was observed both in the tetrapeptides (9.07 ppm at pH 7.2, Figures 3a and 3c; 9.00 ppm at pH 6.5, Tables S5-S6) and in the larger tau peptides (9.05 ppm at pH 7.2, Figure 2a). Similar downfield shifts of the H<sup>N</sup> of Trp were also observed in tau R406W variants (Figure 2b, Figures 3b and 3d, Tables S7-S9). Moreover, smaller  ${}^3J_{\square N}$  were observed at the pSer in these peptides (Figure 3, Table S12; TpSPW, pSer<sub>cis</sub>404,  ${}^3J_{\square N}$  = 5.5 Hz), consistent with a more compact conformation at pSer.<sup>106</sup> In phosphorylated peptides with the *cis*-Pro405 conformation, the downfield chemical shift at R406 or W406, the smaller  $J_{\square N}$  at pSer404, and the inherent preference for an *endo* ring pucker in *cis*-Pro, which promotes a  $\Box$  (–90, 0) conformation at Pro, combine to suggest that Ser404 phosphorylation might induce a type VI  $\Box$ -turn centered at pSer404-Pro405. A type VIa1  $\Box$ -turn conformation was indeed a local energy minimum observed in the geometry-optimized model of Ac-pSer<sup>2-</sup>-*cis*-Pro-NHMe (Figure 7b), suggesting that this

conformation might be inherently promoted in pSer-*cis*-Pro structures. In addition to the effects of phosphorylation on the *cis*-Pro conformation, phosphorylation at Ser404 also resulted in downfield shifts and backbone ordering in the pSer *trans*-Pro amide conformation ( $tau_{395-411}$ -R406: pSer404  $\square$  = 8.67 ppm,  ${}^3J_{\square N}$  = 3.9 Hz; TpSPR: pSer404  $\square$  = 8.74 ppm,  ${}^3J_{\square N}$  = 4.3 Hz), consistent with a pSer404 intraresidue phosphate-amide hydrogen bond that is inherently promoted by phosphorylation. Collectively, these data indicate that Ser404 phosphorylation increases the population of *cis* amide bond and results in ordering in *both* the *trans*-Pro and the *cis*-Pro amide conformations. Moreover, the effects of phosphorylation on structure were present in peptides with the native tau sequence, and were even greater in tau peptides with Trp at residue 406.

Phosphorylation at Ser-Pro or Thr-Pro sequences has previously been observed to increase the activation barrier (reduce the rate of interconversion) for proline *cis-trans* isomerization.<sup>45,53</sup> The larger activation barrier for *cis-trans* isomerization emphasizes the importance of the phosphorylation-dependent prolyl isomerase Pin1 in diverse biological processes. Pin1 is specifically implicated in the phosphorylation-dependent aggregation of tau.<sup>46,47,157,160</sup> However, the basis for slower *cis-trans* isomerization in pSer-Pro sequences is not well understood. By NMR spectroscopy, across multiple peptides, we observed downfield shifts in the *cis*-Pro H□ as a result of phosphorylation, with greater downfield shifts in the dianionic state of pSer. Bioinformatics analysis of Glu-*cis*-Pro structures in the PDB revealed that the Glu carboxylate is frequently positioned close to the Pro H□. Computational investigation of these structures indicated a substantial stabilization of these structures via a Pro-Glu C-H/O interaction. These structures were used to develop a computational model of a pSer-*cis*-Pro structure, which is stabilized by a highly favorable Pro C-H□/phosphate C-H/O interaction

(Figure 7). C–H/O interaction strength is increased by greater partial negative charge (greater electron density) on the oxygen. Thus, a pSer-*cis*-Pro or a pThr-*cis*-Pro C–H/O interaction should be stronger than a Glu-*cis*-Pro C–H/O interaction when the phosphorylated amino acid is in the dianionic ionization state that is predominant at physiological pH. This conclusion is supported experimentally by the increased population of *cis* amide bond and the more downfield Pro H□ chemical shift that was observed in peptides with dianionic pSer.

These data, combined with prior results, indicate that pSer can stabilize both the *trans*Pro conformation (via an intraresidue phosphate-amide hydrogen bond that results in increased order) and the *cis*-Pro conformation (via a Pro C–H□/phosphate C–H/O interaction) (Figure 10). The stabilization of both the *trans* and *cis* conformations, with greater stabilization of the *cis*proline conformation (as reflected in the increased population of *cis* amide bond), provides a structural basis for the observed increased activation barrier of proline *cis-trans* isomerization at pSer-Pro or pThr-Pro sites.

Thus, herein we propose a novel basis for the higher activation barrier due to phosphorylation as SP and TP sites: phosphorylation stabilizes both the *trans*-Pro and *cis*-Pro ground state conformations via favorable interactions, without affecting the transition state energy. Phosphorylation stabilizes the *trans*-Pro conformation via an intraresidue phosphate-amide hydrogen bond. Phosphorylation also stabilizes the *cis*-Pro conformation via a C–H/O interaction between the phosphate and Pro C–H $\Box$ , identified herein (Figures 6-8). Notably, this C–H/O interaction is not geometrically plausible in the transition state for proline *cis-trans* isomerization, where the proline must be rotated ~ 90° relative to the *trans* ( $\omega$  = 180°) or *cis* ( $\omega$  = 0°) conformation. This phosphorylation-dependent decrease in the rate of proline *cis-trans* isomerization is of broad importance, including in transcription by RNA Polymerase II and in

cell cycle progression, as indicated by the diverse substrates of the phosphorylation-dependent prolyl isomerase Pin1.<sup>59,161-166</sup>

Toward models to understand how Ser404 phosphorylation and the R406W modification could increase tau aggregation. Protein aggregation in Alzheimer's disease and other tauopathies is inherently conformationally driven. In addition, protein aggregation is fundamentally a kinetics-driven process, with the rate of formation of toxic aggregates implied to be a key factor in the onset of disease. 49,167-169 Thus, modifications that change protein conformation and dynamics would be expected to change protein aggregation kinetics. Herein, we examined the potential roles of Ser404 phosphorylation and the R406W modification in changing local structure in tau. We also examined the effects of the R406W variant on enzymatic modification of tau, using well-studied tau kinases and phosphatases, including the protein kinases cdk5 and GSK-3 and the protein phosphatase PP2A. We observed no significant effect of the R406W modification on phosphorylation by either cdk5 or GSK-3. In addition, the R406W modification should make Ser409 a significantly worse substrate for the kinase PKA and related kinases that prefer an Arg at the -3 position.

Moreover, the R406W modification significantly *increased* tau dephosphorylation by PP2A, at both pSer404 and pSer409. While other kinases and phosphatases could certainly show sequence-dependent changes due to the R406W modification that would increase tau phosphorylation, we found no evidence using the enzymes studied that the R406W modification would increase the phosphate stoichiometry at Ser404 or at Ser409. Indeed, data on PP2A indicated that this enzyme would significantly *reduce* tau phosphorylation in R406W-modified tau.

We therefore examined other mechanisms by which the R406W modification could change tau structure or dynamics. Ser404 phosphorylation is increased in neurodegeneration and disease (as indicated by increased reactivity with the PHF-1 antibody against pSer396/pSer404), and the phosphorylation-dependent prolyl isomerase Pin1 has been implicated in tau aggregation and neurodegeneration. In addition, Ser404 pseudophosphorylation has been observed to change the dynamics of tau aggregation and to change the structure of the tau global hairpin. herein, we observed that both the R406W modification and Ser404 phosphorylation increased the population of *cis*-Pro amide bond in tau peptides. In addition, both the R406W modification and Ser404 phosphorylation increased ordering in the local sequence in both *trans*-Pro405 and *cis*-Pro405 amide conformations. Collectively, these data suggested the possibility (Figure 11) that *cis-trans* isomerization at Pro405 might be important in *tau* structure and dynamics, via increasing the population of *cis* amide bond, via increasing the activation barrier of Pro405 *cis-trans* isomerization, and via inherent changes in structure in *trans*-Pro versus *cis*-Pro.

Experimental, bioinformatics, and computational analyses all indicated that both Ser404 phosphorylation and the R406W modification had the ability to independently stabilize *both* the *cis* and *trans* Pro amide conformations. The stabilization of the *cis*-Pro and *trans*-Pro ground states, if occurring without a significant impact on the energy of the transition state between these conformations, indicates that a significant effect of both Ser404 phosphorylation and the R406W modification could be to increase the activation barrier of, and thus slow the rate of, Pro405 *cis-trans* isomerization. The broad data implicating the phosphorylation-dependent prolyl isomerase Pin1 in tau pathology in AD suggest that both modifications might be relevant to the kinetics and molecular mechanisms of tau structural changes and aggregation in AD and other tauopathies.<sup>46,49,58</sup>

Tau adopts a dynamic global hairpin conformation, in which both the N-terminal and C-terminal regions fold over the hydrophobic and aggregation-prone microtubule-binding domain.<sup>27</sup> The proline-rich domain and C-terminal domain of tau contain most of the phosphorylation sites that are observed in disease. These regions of tau, and their phosphorylation sites, are not part of the ordered regions of tau aggregates.<sup>21-24</sup> As such, alternative models must be developed to explain how phosphorylation in these domains might play a mechanistic role in tau aggregation. The global hairpin model provides a context for potentially understanding these effects. We have previously shown that phosphorylation in the tau proline-rich domain induces disorder-to-order transitions, including induced local polyproline II helix (PPII) conformation.<sup>38-40</sup> Herein, we demonstrate that both Ser404 phosphorylation and the R406W modification increase the population of Pro405 *cis* amide bond, either independently or in combination, via a pSer-*cis*-Pro C–H/O interaction and/or an H□-*cis*-Pro-aromatic C–H/□ interaction.

A *cis*-proline conformation inherently produces a []-turn-like conformation, by bringing the *i* and *i*+3 residues in close proximity.<sup>150</sup> The kinking induced by a *cis*-Pro amide bond, compared to a *trans*-Pro amide bond,<sup>156</sup> could potentially impact the dynamics of the global hairpin, most significantly via changes in the ability of the C-terminal domain to fold against the TBD and protect it from aggregation (Figure 12). Proline *cis-trans* isomerization can induce large structural changes in proteins, and a change in the exposed hydrophobic surface area of the TBD could drive self-association to generate the thermodynamically favored tau aggregates. Notably, similar effects in increasing the population of the *cis*-proline conformation as a result of serine phosphorylation are also possible at other Ser-Pro sites, including Ser396 and Ser422 in the C-terminal domain and Ser199, Ser202, and Ser235 in the proline-rich domain. Alternatively,

the R406W mutation, potentially enhanced by Ser404 phosphorylation, could also promote local order and turn conformations with *trans*-proline, similarly inducing kinking in the tau C-terminal domain.

Collectively, the data herein indicate that the R406W modification in tau is expected to have the following effects: (1) increased hydrophobicity; (2) increased population of *cis*-Pro amide bond; and (3) increased population of turn conformations in both the *trans* and *cis* Pro amide conformations. Moreover, phosphorylation of Ser404 would increase the activation barrier for Pro405 *cis-trans* isomerization (slower conversion from *cis* to *trans* amide bond and *vice versa*). These results provide a basis for further studies on the molecular mechanisms of tau misfolding and aggregation.

#### **Conclusion**

We have examined a series of potential mechanisms by which the tau R406W mutation could result in the increase in tau aggregation and neurodegeneration that is observed both in the human tauopathy FTDP-17 and in animal models of Alzheimer's disease. We found in  $tau_{395.411}$  peptides that the R406W modification does not significantly increase phosphorylation at Ser404 by cdk5/p35 or by GSK-3. In addition, based on kinase substrate specificity data, the R406W mutation should significantly reduce phosphorylation at Ser409 by protein kinase A and other protein kinases that prefer Arg at the P-3 position (here, residue 406). Moreover, surprisingly, the R406W modification significantly *increased* tau dephosphorylation by the protein phosphatase PP2A. These data suggest that increased levels of phosphorylation at Ser404 or Ser409 via the enzymes examined are unlikely to explain the effect of tau R406W modification on tau aggregation. The R406W modification results in the replacement of a charged amino acid

with a highly hydrophobic, aromatic amino acid, which could inherently increase aggregation, although this residue is outside the aggregation-prone microtubule-binding domain. In addition, we observed that the R406W modification in tau peptides results in an increase in population of cis-Pro amide bond at Pro405. Trp interacts to stabilize both the cis and trans Pro amide conformations via C−H/□ interactions of the Trp aromatic ring with H□ of the pre-Pro residue (here, Ser404) and/or with  $H \square$  or  $H \square$  of the proline ring. In addition, we found that Ser404 phosphorylation significantly increases the population of cis-Pro at the pSer-Pro amide bond, with effects that are additive to those of the R406W modification in increasing cis amide bond. We propose that pSer-cis-Pro amide bonds are stabilized via a C-H/O interaction between the pSer phosphate and the Pro C-H[]. C-H/O interactions were observed broadly in Glu-cis-Pro sequences in the PDB. Pro-phosphate C-H/O interactions that stabilize the cis-Pro amide conformation, in combination with intraresidue phosphate-amide hydrogen bonds that stabilize the trans-Pro amide conformation, are proposed to be the primary mechanism by which phosphorylation at Ser and Thr increases the activation barrier for proline cis-trans isomerization.

# **Experimental**

**Peptide synthesis and characterization**. All peptides were synthesized via solid-phase peptide synthesis using Rink amide MBHA resin. Peptides were acetylated at the N-termini and contained C-terminal amides. Peptides were purified to homogeneity and were characterized via <sup>1</sup>H NMR and mass spectrometry. Detailed synthetic procedures and characterization of the peptides are in the Supporting Information.

<sup>1</sup>H NMR spectroscopy. All <sup>1</sup>H NMR spectra were acquired on a Brüker AVC 600 MHz spectrometer with a triple resonance cryoprobe or a TXI probe. Peptides were allowed to dissolve in a solution containing 5 mM phosphate buffer (with pH adjusted to 4.0, 6.5, 7.2, 8.0, or 8.5 as indicated), 25 mM NaCl, and 0.1 mM TSP in 90%  $H_2O/10\%$   $D_2O$ . Water suppression was achieved with an excitation sculpting pulse sequence for all NMR spectra. TOCSY spectra were used for resonance assignment, and were acquired with 2048 data points and 512  $t_1$  increments, with 8 scans per  $t_1$  increment.

**PDB analysis**. The protein data set for analysis was constructed using the PISCES server. The protein the PDB were chosen that were solved by X-ray crystallography with a resolution  $\leq 2.0 \text{ Å}$ , R-factor  $\leq 0.25$ , and sequence identity  $\leq 25\%$ . The data set includes 5974 protein chains. In-house scripts and the external program Pymol were used for structure analysis. Dihedral angles of  $-90^{\circ} < \square < +90^{\circ}$  were defined as a *cis*-proline conformation, while dihedral angles with  $|\square| > 150^{\circ}$  were defined as a *trans*-proline conformation.

Computational analysis. Protein structures from the PDB were truncated to minimal Glu-cis-Pro structures via the following general approach. Hydrogens were added to protein structures using Pymol. The resultant all-atom protein structures were reduced to tripeptide or tetrapeptide fragments within Pymol. These peptide fragments were further reduced in size to

tripeptides or to minimalist bimolecular complexes within GaussView 5.<sup>136</sup> In order to accurately position the hydrogens, a restrained geometry optimization was performed on the resultant structures, in which the crystallographically determined positions of the heavy atoms were fixed and the positions of the hydrogens were optimized, with final geometry optimization conducted with the M06-2X method and the 6-311++G(2d,2p) basis set. Further details are in the Supporting Information. These structures were analyzed via energy, counterpoise, and/or natural bond orbital (NBO)<sup>142</sup> analysis, as appropriate, using the MP2 method and the 6-311++G(3d,3p) and aug-cc-pVTZ basis sets.<sup>137-139</sup> Counterpoise calculations in vacuum were used to quantify gas-phase interaction energies and basis-set superposition energies (BSSE). All other calculations were conducted in implicit water (IEFPCM continuum polarization model). Quantitative analysis of NBO energies and complex interaction energies in implicit water, as well as additional discussion, is in the Supporting Information.

A model of a pSer-cis-Pro structure was generated using geometries observed in Glu-cis-Pro structures with a C-H/O interaction that were in the PDB. The peptide Ac-pSer-cis-Pro-NHMe was modeled with an initial geometry of dianionic pSer in the polyproline II helix conformation and a  $g^ \chi_1$  torsion angle. The proline initial geometry included an *endo* ring pucker and  $\phi$  and  $\psi$  torsion angles of (-90°, 0°). This structure was subjected to geometry optimization using the M06-2X DFT functional<sup>140</sup> and the 6-311++G(d,p) basis set in implicit water. The resultant structure was subsequently subjected to additional geometry optimization with the 6-311++G(2d,2p) basis set, then further optimization with the 6-311++G(3d,3p) basis set. The resultant structure was analyzed via a frequency calculation, which indicated no imaginary frequencies. This model was then used to generate a minimalist methylphosphate<sup>2-</sup>
•For-Pro-NH<sub>2</sub> complex, which was used for subsequent analysis of complex interaction energy,

using methods as had been employed for acetate • For-Pro-NH<sub>2</sub> complexes. Additional details are in the Supporting Information.

Models of  $tau_{404-406}$ –R406W peptides with pSer404 were generated initially from PDB lobb, with Glu changed to pSer<sup>2-</sup>. This model was subjected to iterative geometry optimization, with the final geometry optimization conducted with the M06-HF DFT functional in implicit water (IEFPCM), using the Def2TZVP basis set on all heavy atoms the Def2SVP basis set on hydrogens. Relevant torsion angles were then rotated on this structure to match different conformations observed in pSer and/or in Pro-Trp structures in the PDB, and those resultant initial models subjected to full geometry optimization using the same methods. These structures were analyzed within GaussView and Pymol for torsion angles and potential stabilizing noncovalent interactions. Coordinates of all geometry-optimized structures are in the Supporting Information.

Phosphorylation by GSK-3 and cdk5/p35. Comparative phosphorylation rates of the peptides  $tau_{395-411}$  R406 pS409 and  $tau_{395-411}$  R406W pS409 with GSK-3 were determined in a solution with 150  $\mu$ M peptide substrates containing 20 mM HEPES (pH 7.5), 100 mM NaCl, 4 mM MgCl<sub>2</sub>, 1.2 mM DTT, 0.5  $\mu$ M glycerolphosphate, 10  $\mu$ M Na<sub>3</sub>VO<sub>4</sub>, and 40  $\mu$ g/mL BSA. Similarly, for the peptides  $tau_{395-411}$  S404 R406 and  $tau_{395-411}$  S404 R406W comparative phosphorylation rates with cdk5/p35 were determined with 100  $\mu$ M peptide substrates in a solution containing 20 mM HEPES (pH 7.5), 100 mM NaCl, 3 mM MgCl<sub>2</sub>, 3 mM MnCl<sub>2</sub>, 1.2 mM DTT, 0.5  $\mu$ M glycerolphosphate, 10  $\mu$ M Na<sub>3</sub>VO<sub>4</sub>, and 40  $\mu$ g/mL BSA. The solutions were allowed to incubate at 37 °C for 45 minutes prior to the addition of ATP (1.5 mM, final concentration) and the kinase (0.4  $\mu$ g of GSK-3 or 0.6  $\mu$ g of cdk5/p35) at the start of the experiment. Aliquots (10  $\mu$ L) of the reaction mixtures were analyzed on the HPLC. Identities of

the peptides were verified via coinjection of the reaction mixtures with the independently synthesized peptides and/or via mass spectrometry. Detailed procedures and the results of the experiments are in the Supporting Information.

**Dephosphorylation by PP2A**. Comparative dephosphorylation rates of the peptides  $tau_{395-411}$  pS404 R406,  $tau_{395-411}$  pS404 R406W,  $tau_{395-411}$  R406 pS409, and  $tau_{395-411}$  R406W pS409 were determined with 100 μM peptide substrates in a solution containing 20 mM MOPS (pH 7.4) 100 mM NaCl, 60 mM 2-mercaptoethanol, 1 mM MgCl<sub>2</sub>, 1 mM EGTA, 0.1 mM MnCl<sub>2</sub>, 1 mM DTT, 10% glycerol, and 0.1 mg/mL serum albumin. The solutions were allowed to incubate at 37 °C for 45 minutes prior to the addition of the phosphatase (0.1 units). Aliquots (10 μL) of the reaction mixtures were quenched with 10 nM okadaic acid and were analyzed via HPLC. Identities of the peptides were verified via coinjection of the reaction mixtures with the independently synthesized peptides and via mass spectrometry. Detailed procedures and the results of the experiments are in the Supporting Information.

# Acknowledgements

We thank the DOD CDMRP PRARP program (AZ140115), NSF (MCB-1616490), and NIH (GM093225) for funding. Instrumentation support was provided by NIH (GM110758) and NSF (CHE-1229234).

# **Supporting Information Available**

Synthesis and characterization data of all peptides, data for kinase and phosphatase experiments, additional 1-D and 2-D NMR spectra, tabulation of NMR data, additional bioinformatics data, computational methods and results, coordinates of geometry-optimized compounds. This material is available free of charge via the Internet at the journal web site.

# **Figures**

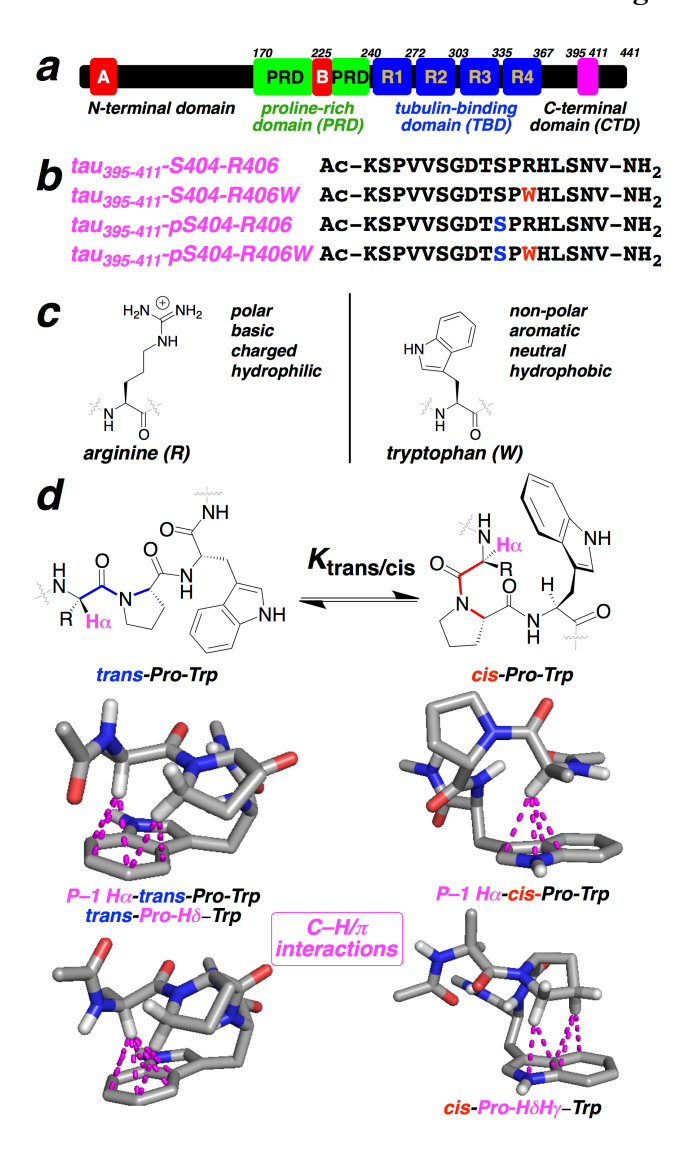


**Figure 1**. (a) Domain architecture of the largest isoform of tau. Tau binds microtubules via the tubulin-binding domain (TBD), which consists of 4 microtubule-binding repeats (R1–R4, blue). The TBD is preceded by two proline-rich segments collectively termed the proline-rich domain (PRD, green). The N-terminal domain (residues 1–170) and the PRD have hydrophobic regions (red), indicated as A and B, respectively. In the C-terminal domain (CTD), within the 17-residue sequence from residues 395-411 ( $tau_{395-411}$ , magenta), the PHF-1 epitope sites Ser396 and Ser404 and the R406W mutation site are in close proximity. Both Ser396 and Ser404 precede Pro residues. (b) Amino acid sequences and modifications in  $tau_{395-411}$  peptides examined herein. Phosphorylated residues are indicated in blue. The R406W modification site is indicated in red. (c) The tau R406W modification involves the change of a polar, charged amino acid (Arg) to an uncharged, hydrophobic, aromatic amino acid (Trp). (d) In a Pro-Trp sequence, Trp can stabilize structures in the *trans*-Pro or the *cis*-Pro amide conformation, via a C–H/□ interaction of the Trp indole with the H□ of the residue preceding the proline (H□-Pro-Trp C–H/□ interaction) and/or with the H□, H□, and/or H□ of the proline ring (Pro-H-Trp C–H/□ interaction). These

interactions are observed to stabilize secondary structures, loops, and  $\Box$ -,  $\Box$ -, and  $\Box$ -turn geometries. In addition to C–H/ $\Box$  interactions, these structures can also be stabilized via the hydrophobic effect. Representative Pro-Trp structures that stabilize (*trans*) type I  $\Box$ -turns and (*cis*) type VIa1  $\Box$ -turns are shown. Additional examples are in ref. In general, the interactions with the pre-proline (P–1) residue H $\Box$  are more favorable than interactions on Pro, but these P–1 C–H $\Box$ / $\Box$  interactions require two disfavored conformations (e.g. *cis*-proline,  $\Box$ L or \* at the P–1 residue or Trp,  $g^+$  Trp  $\chi_1$ ). The observation of interactions at P–1 indicate that the Trp can promote conformations that are inherently disfavored or that typically represent infrequent native populations.

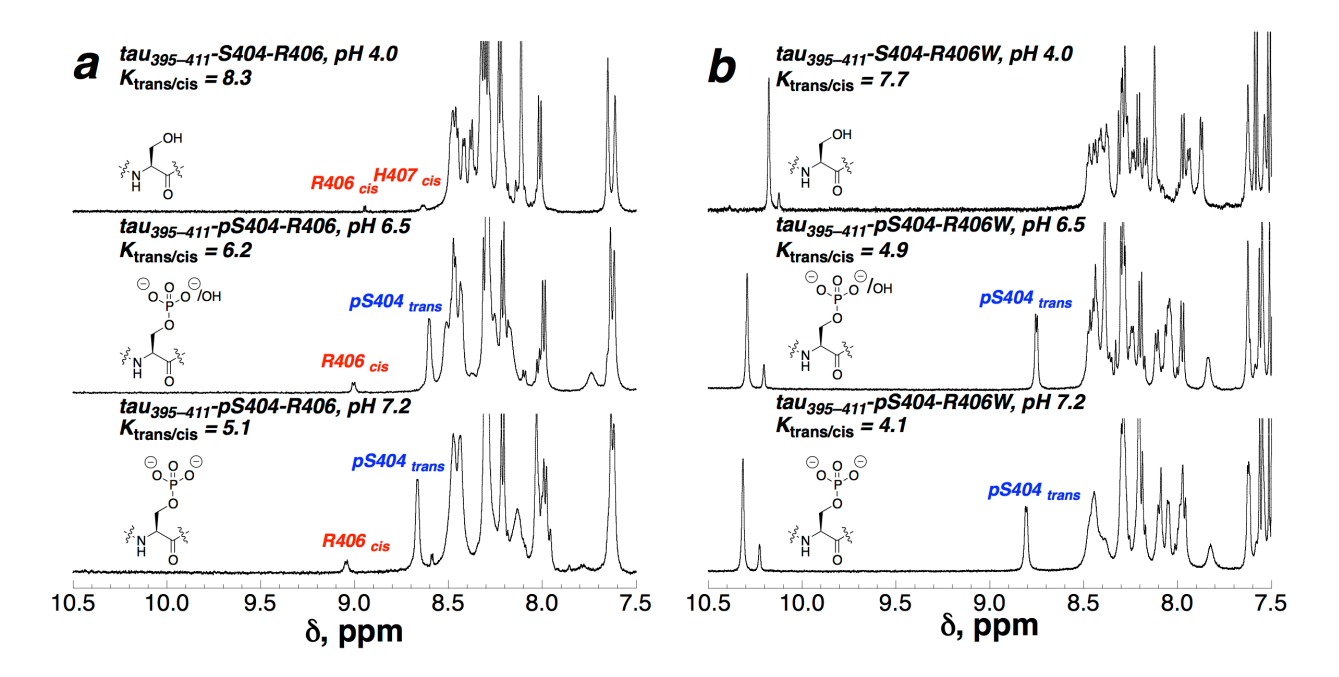


**Figure 2**. Effects of phosphorylation at Ser404 on *cis-trans* isomerization of Pro405 in  $tau_{395-411}$  peptides with (a) Arg406 and (b) Trp406. Amide region of the <sup>1</sup>H NMR spectra of the  $tau_{395-411}$  peptides with (top to bottom) non-phosphorylated Ser404 (pH 6.5), phosphorylated Ser404 at pH 6.5, and phosphorylated Ser at pH 7.2 (dianionic pSer). The spectra were obtained with peptide in a solution with 5 mM sodium phosphate and 25 mM sodium chloride in 90% H<sub>2</sub>O/10% D<sub>2</sub>O at 298 K. Phosphorylation at Ser404 in  $tau_{395-411}$  (a) with the native Arg406 and (b) with the R406W modification induces the *cis* amide conformation. (b) The R406W modification combined with the Ser404 phosphorylation substantially increases the *cis*-Pro405 conformation in the peptides derived from  $tau_{395-411}$ .  $K_{trans/cis}$  = [population of peptide with *trans* amide bond]/[population of peptide with *cis* amide bond], determined via integration of the areas of the peaks representing the *trans* and *cis* Pro amide rotamers. A smaller  $K_{trans/cis}$  indicates a higher population of *cis*-Pro.

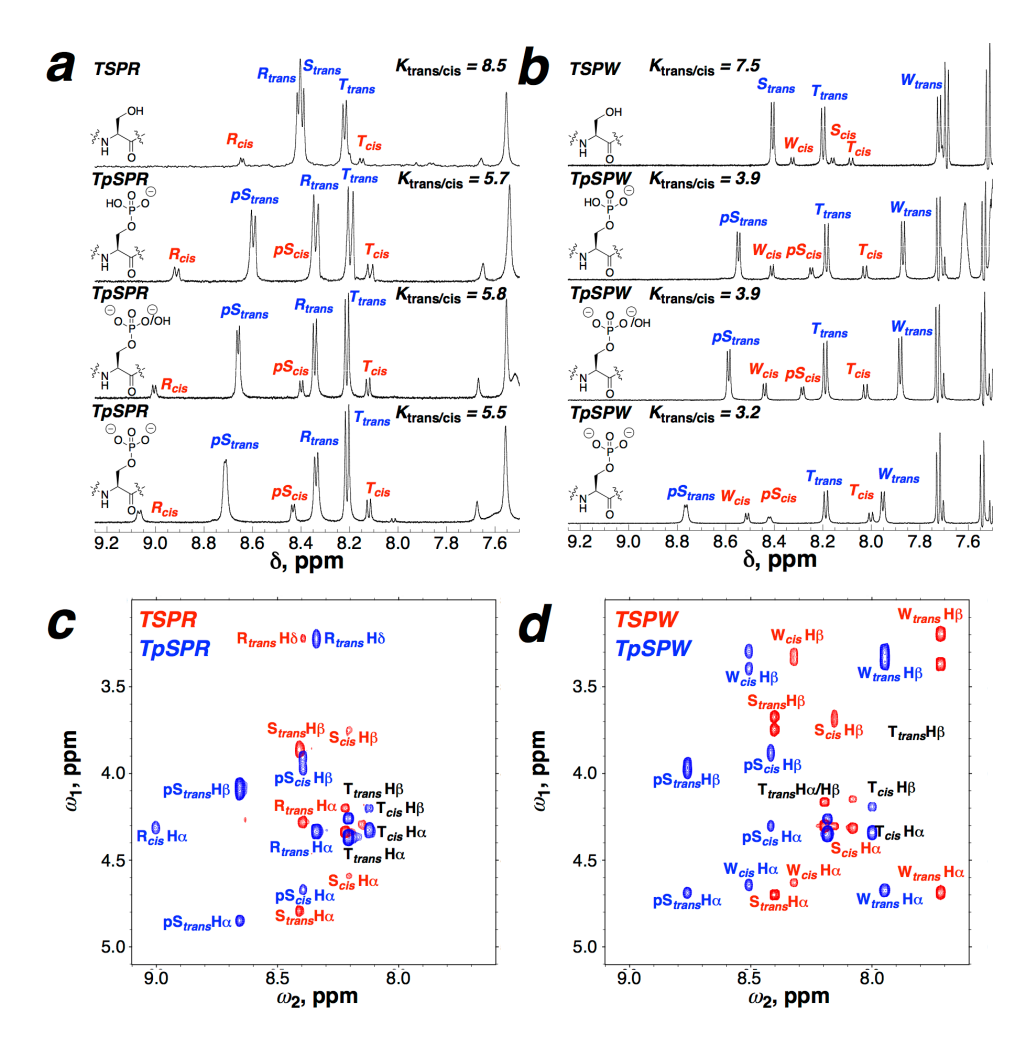


**Figure 3**. Effects of phosphorylation at Ser404 with (a) Arg406 or (b) Trp406 on *cis-trans* isomerization of Pro405 in the  $tau_{403-406}$  peptides, Ac-TSPX-NH<sub>2</sub>. Amide region of the <sup>1</sup>H NMR spectra of the peptides (a) Ac-TSPR-NH<sub>2</sub> and (b) Ac-TSPW-NH<sub>2</sub>, with (top to bottom) non-phosphorylated Ser (pH 4.0) and phosphorylated Ser (pS) at pH 4.0, 6.5, and 7.2. (c) Superposition of the TOCSY spectra of the peptides TSPR (red) and TpSPR (blue), at pH 4.0 and 6.5, respectively. (d) Superposition of the TOCSY spectra of the peptides TSPW (red) and TpSPW (blue), at pH 4.0 and 7.2, respectively. The spectra were obtained with peptide in a solution with 5 mM sodium phosphate and 25 mM sodium chloride in 90% H<sub>2</sub>O/10% D<sub>2</sub>O at 298 K. Both phosphorylation at Ser and the R406W modification induce a *cis*-Pro conformation, similar to observations in the larger  $tau_{395-411}$  peptides.

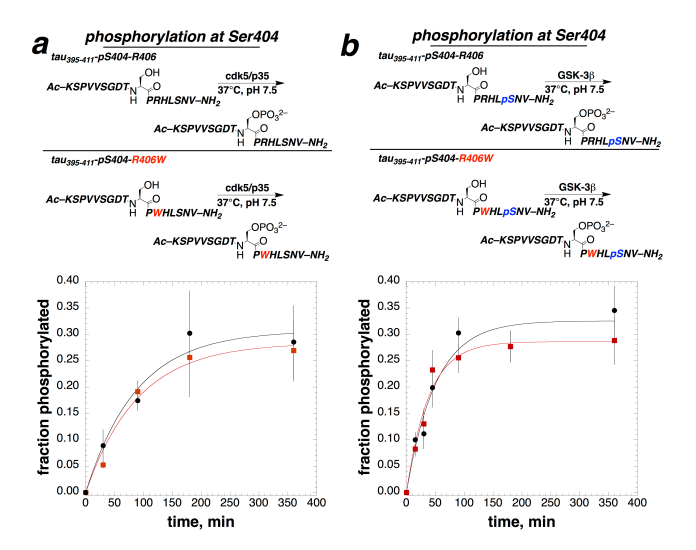


**Figure 4.** Enzymatic phosphorylation of  $tau_{395-411}$  peptides. Phosphorylation of  $tau_{395-411}$  at Ser404 (a) by cyclin-dependent kinase-5 (cdk5/p35) and (b) by glycogen synthase kinase-3 (GSK-3) at 37 °C. (a) Phosphorylation of Ser404 by cdk5/p35 in  $tau_{395-411}$  peptides with R406 (black circles) and with the R406W modification (red squares) ( $k_{rel} = 1.0 \pm 0.9$ ). (b) Phosphorylation of Ser404 by GSK-3 in  $tau_{395-411}$  peptides phosphorylated at Ser409, in peptides with R406 (black circles) and with the R406W modification (red squares) ( $k_{rel} = 1.3 \pm 0.2$ ). Data were fit to a pseudo-first order rate equation.  $k_{rel} = (rate constant for the peptide with R406W modification)/(rate constant for the peptide with Arg at residue 406). Error bars indicate standard error from at least three independent trials.$ 

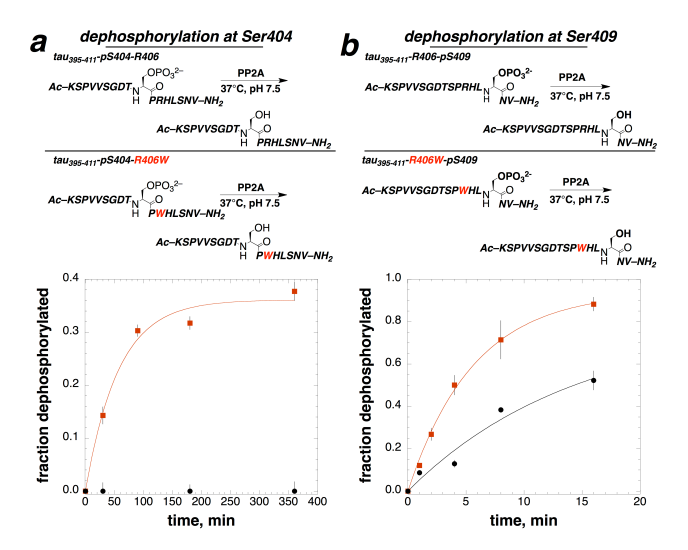


**Figure 5**. Enzymatic dephosphorylation of  $tau_{395-411}$  peptides at (a) pSer404 and (b) pSer409 by protein phosphatase 2A (PP2A) at 37 °C. (a) Dephosphorylation of pSer404 with R406 (black circles) and with the R406W modification (red squares) in  $tau_{395-411}$ . (b) Dephosphorylation of pSer409 with R406 (black circles) and with the R406W modification (red squares) in  $tau_{395-411}$ . The R406W modification in  $tau_{395-411}$  increases the rate of dephosphorylation at both the pSer404 ( $k_{\rm rel} > 1000$ ) and the pSer409 ( $k_{\rm rel} = 2.5 \pm 0.3$ ) sites.  $k_{\rm rel} = ({\rm rate constant for the peptide with the R406W modification})/({\rm rate constant for the peptide with Arg at residue 406})$ . In addition, in  $tau_{395-411}$  with the R406W modification, PP2A more rapidly dephosphorylates Ser409 compared to Ser404 ( $k_{\rm rel} = 4.1 \pm 0.8$ ). Data were fit to a pseudo-first order rate equation. Error bars indicate standard error from at least three independent trials.

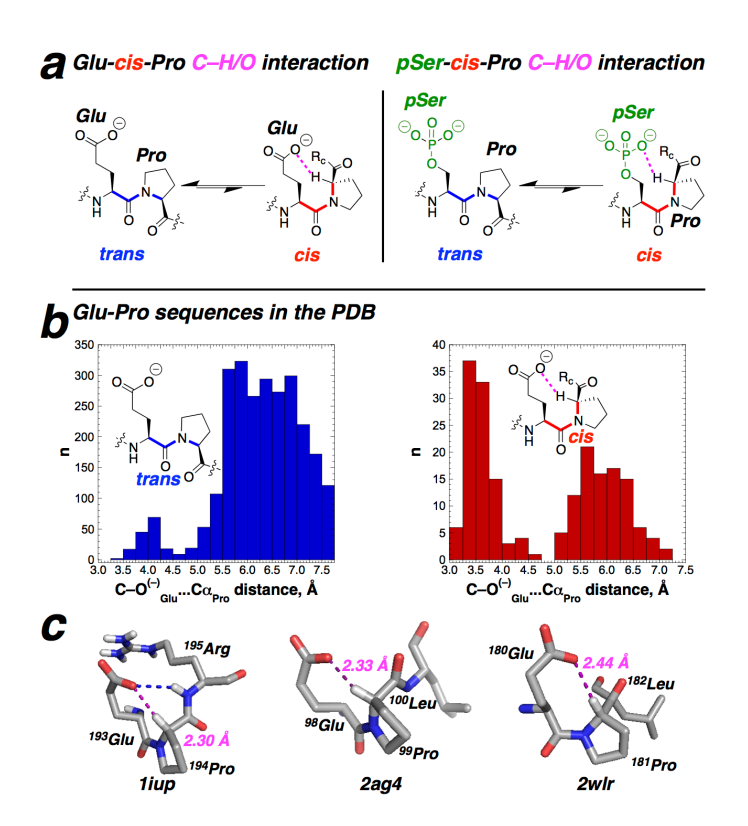


**Figure 6**. C–H/O interactions stabilize the *cis*-Pro conformation in Glu-*cis*-Pro and pSer-*cis*-Pro structures. (a) Pro C–H $\square$ /Glu C–H/O interactions observed in Glu-*cis*-Pro structures in the PDB and the proposed analogous Pro C–H $\square$ /phosphate C–H/O interaction. (b) Distances from proline C $\square$  to the Glu side chain O closest to Pro C $\square$  (C–O $^{(-)}$ <sub>Glu</sub>····C $\square$ <sub>Pro</sub> distance). 48% of Glu-*cis*-Pro structures in the PDB exhibit a C–H/O interaction, while only 5% of the Glu-*trans*-Pro structures exhibit a C–H/O interaction. (c) Representative examples of Glu-*cis*-Pro structures exhibiting a C–H/O interaction, with the H $\square$ ···O distance indicated. Hydrogens were added in Pymol, followed by geometry optimization of the positions of the hydrogens by DFT methods; see the Supporting Information for details.

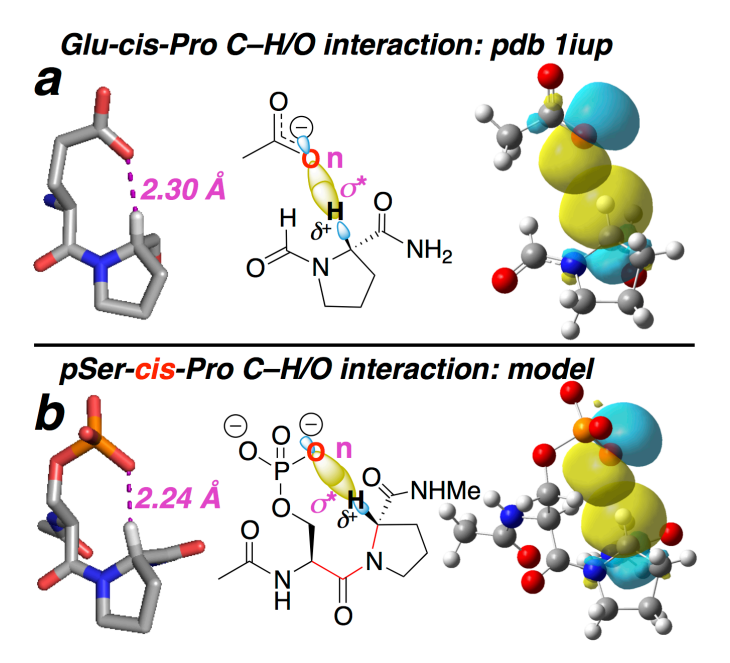
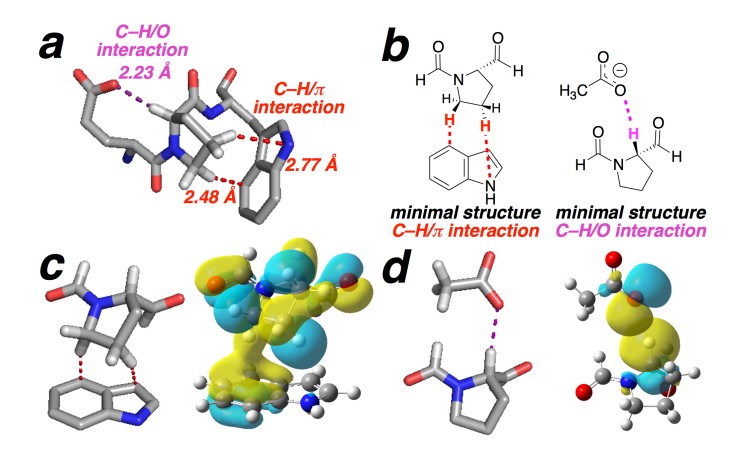


Figure 7. C-H/O interactions stabilizing the cis-Pro conformation in Glu-Pro and pSer-Pro sequences. (a) (left) Glu-cis-Pro conformation from PDB liup, a hydrolase protein from Pseudomonas fluorescens (residues 193-194);<sup>171</sup> (center) minimalist structure used for determination of complex interaction energies; (right) natural bond orbital (NBO) analysis of the C-H/O interaction, showing orbital overlap between one carboxylate lone pair and the C-H $\square$ orbital contributing to interaction stabilization. Energy calculations on a minimal AcO-•For-Pro-NH<sub>2</sub> structure derived from 1 iup indicated a corrected interaction energy in implicit water of – 2.1 kcal mol<sup>-1</sup>. Glu-cis-Pro structures had similar C-H/O interaction energies in other representative examples, including pdb 2wlr (residues 180-181) and pdb 2ag4<sup>172</sup> (residues 98-99), with -1.5 kcal mol<sup>-1</sup> and -2.1 kcal mol<sup>-1</sup> interaction energies, respectively. (b) Geometryoptimized pSer-cis-Pro structural model in Ac-pSer-cis-Pro-NHMe. pSer adopts the PPII conformation (-59°, +145°) with a  $g^- \chi_1$  torsion and with  $\chi_2 = -94$ °. Pro is in the  $\delta$  conformation (-93°, +20°) with an *endo* ring pucker. The overall structure adopts a type VIa1 ∏-turn (PcisD), with a 1.98 Å turn hydrogen bond. This structure was one of multiple geometries identified in which a Pro C-H\(\pi\)epSer C-H\(\text{O}\) interaction stabilized cis-Pro. Right: NBO analysis of the C-H/O interaction, showing the molecular orbital overlap between one phosphate lone pair and the  $C-H \cap \Gamma^*$  molecular orbital, which contributes to interaction stabilization via electron delocalization. The geometry of Ac-pSer-Pro-NHMe was optimized using the M06-2X functional and the 6-311++G(3d,3p) basis set in implicit water. This structure was then further reduced to a MeOPO<sub>3</sub><sup>2</sup>-•For-Pro-NHMe complex, for the calculation of complex interaction energies. The stabilization energy of the MeOPO<sub>3</sub><sup>2</sup>•For-Pro-NHMe complex was -3.0 kcal mol<sup>-</sup> <sup>1</sup>. All energy calculations were performed at the MP2 level of theory using the aug-cc-pVTZ basis set in implicit water. Interaction energies were corrected using gas-phase BSSE, as determined by counterpoise calculations.



**Figure 8.** Dual C–H/O and C–H/ $\square$  interactions stabilizing the *cis*-Pro conformation in pdb 10bb. (a) The Glu-cis-Pro-Trp structure from the protein ∏-glucosidase (pdb 1obb, residues 282-284, 1.9 Å resolution). The cis-Pro conformation is stabilized via two interactions: (1) a C-H/O interaction between the Glu side chain O and C-H of Pro (magenta); and (2) a C-H/ interaction between the Trp indole side chain and  $H \square$  and  $H \square$  of cis-Pro (red). (b) Minimal structures derived from the crystallographic coordinates of pdb 1obb. (left) The For-Pro-H•indole complex represents a minimal cis-ProH∏/H□••Trp C–H/□ interaction. (right) The AcO-•For-Pro-H complex represents a minimal Glu-cis-ProH C−H/O interaction. (c) The corrected Pro•indole interaction energy was -6.0 kcal mol<sup>-1</sup>, on the minimalist For-Pro-H•indole complex. The C-H/∏ interaction includes delocalization of electrons between the indole ∏ molecular orbitals and the  $C-H \square$  and/or  $C-H \square \square^*$  molecular orbitals of Pro to stabilize the complex. (d) The corrected interaction energy calculated for the AcO-•For-Pro-H complex was -2.4 kcal mol<sup>-1</sup>. The C-H/O interaction includes the delocalization of electrons between the acetate oxygen and the Pro C-H $\cap$   $\cap$  molecular orbitals to stabilize the complex. Both C-H $\cap$  and C-H $\cap$ interactions include additional stabilization via electrostatic interactions between the anionic oxygen and the partial positive charge ([]\*) on the indicated Pro hydrogens. All energy calculations were conducted using the MP2 method with the aug-cc-pVTZ basis set in implicit water. Additional details of the calculations and the interaction energies are in the Supporting Information.

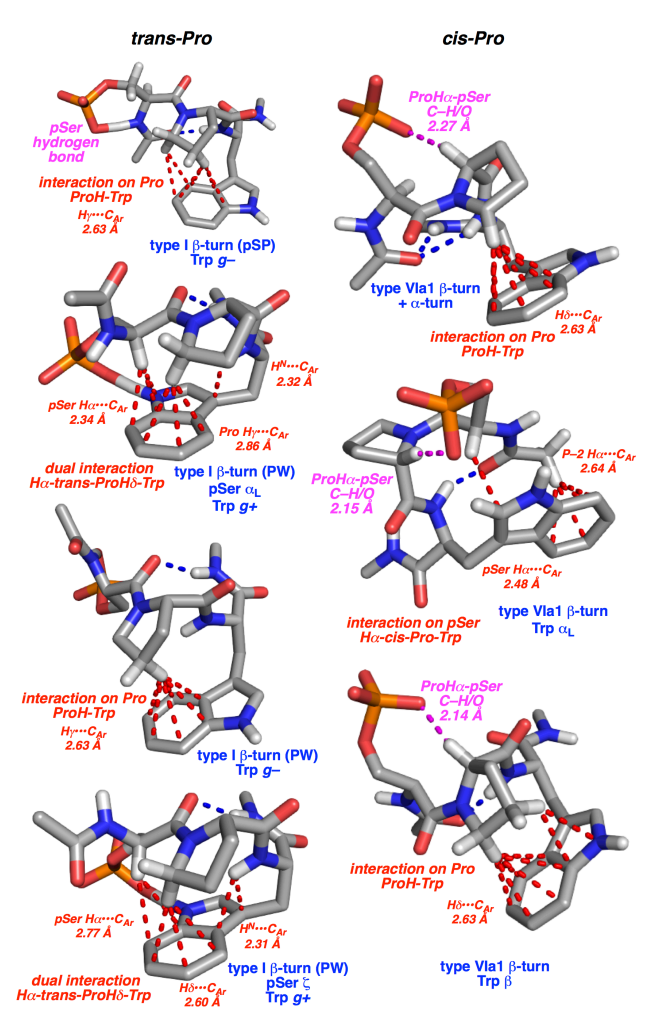
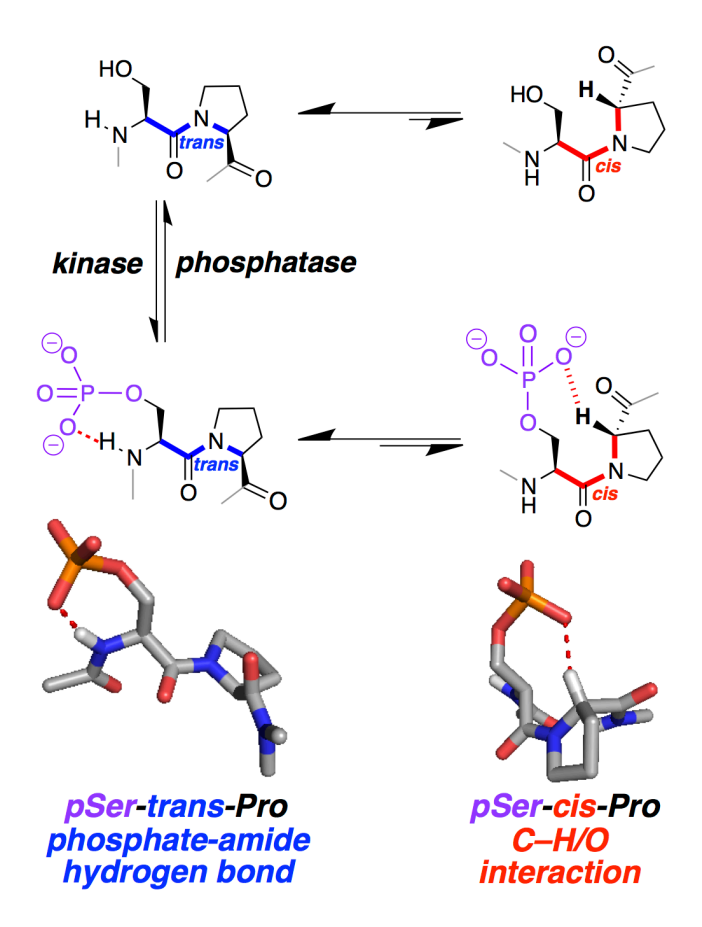
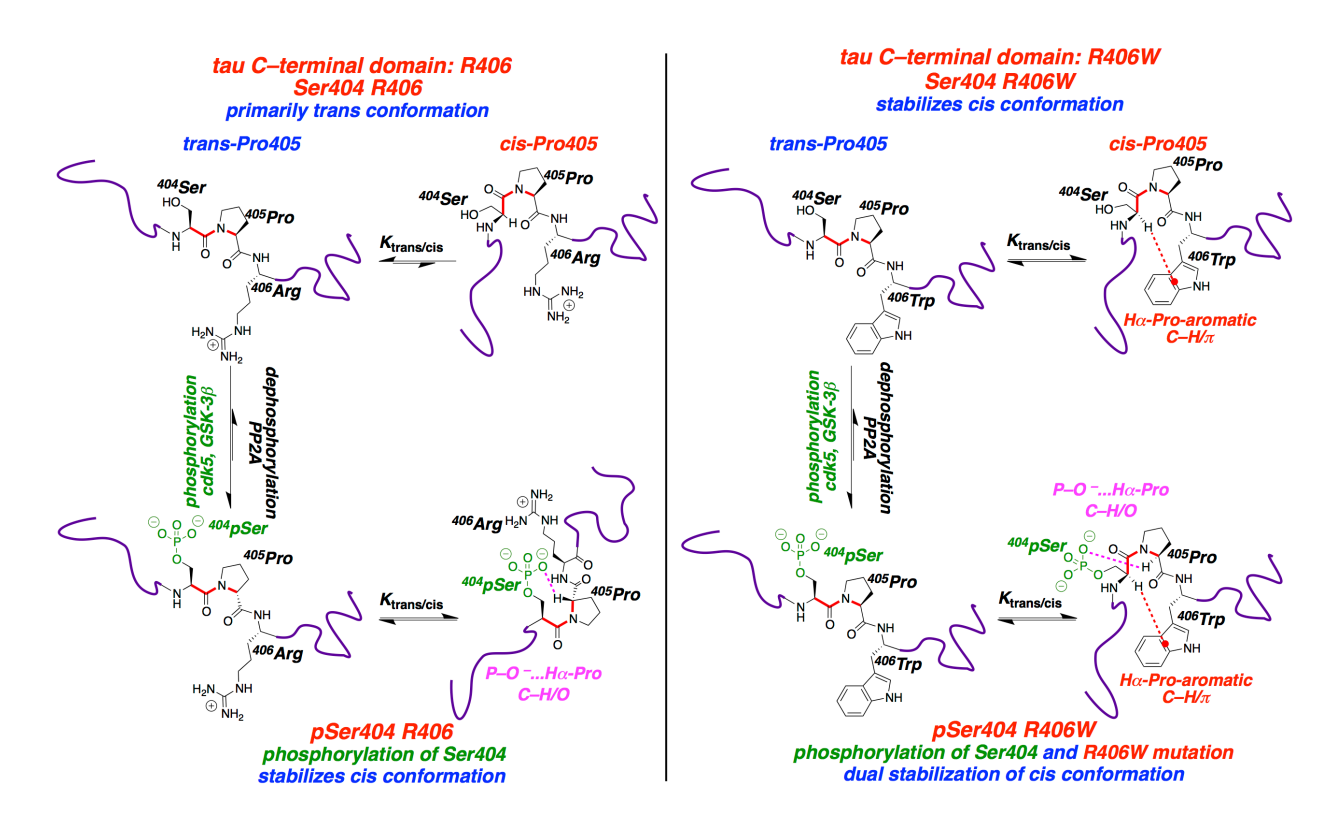


Figure 9. Computational models of non-covalent interactions stabilizing turn conformations in Ac-pSer-Pro-Trp sequences. (left) For trans-Pro, the pSer phosphate may interact favorably in an intramolecular hydrogen bond with its own amide N-H, and the Trp aromatic ring may interact with the Pro ring, with the pSer C–H bonds, or with both simultaneously (dual interaction). The interactions of Trp with pSer specifically can stabilize higher-energy protein conformations (e.g.  $\prod_{L, *, g^+}$ . Type I  $\prod$ -turns centered on either Pro-Trp (PW) and pSer-Pro (pSP) are shown. (right) For *cis*-Pro, the pSer phosphate can interact with Pro H $\square$  to stabilize the *cis*-Pro conformation. The Trp aromatic ring can interact with C-H bonds on Pro or pSer. These structures are meant to be representative structures of \(\preceit\_{\text{turns}}\) with stabilizing non-covalent interactions (hydrogen bonds, C–H/O interactions, and/or C–H/∏ interactions), and do not represent a complete analysis of all possible conformations in these sequences. The structures resulted from geometry optimization using the M06-HF DFT functional, with the Def2TZVP basis set on heavy atoms and the Def2SVP basis set on hydrogens, in implicit water (IEFPCM model). Hydrogen bonds of ∏-turns are indicated in blue. C–H/∏ interactions, with the closest observed H•••C distances at any aromatic carbon (C<sub>Ar</sub>), are indicated in red. C-H/O interactions between the phosphate and Pro H are indicated in magenta. In the structure of pSer-trans-Pro with a pSer-Pro-centered type I ∏-turn, the pSer intraresidue phosphate-amide hydrogen bond, which appears as a covalent bond in the figure, would be expected to strengthen the  $\prod$ -turn hydrogen bond, by making the i residue (Ac-) carbonyl a more electron-rich electron donor for interaction with the i+3 amide N-Η.



**Figure 10**. Ser phosphorylation leads to interactions that are stabilizing in both the *trans* and *cis* amide conformations of pSer-Pro sequences.



**Figure 11**. Model of the effects on tau structure of proline *cis-trans* isomerization and enzymatic phosphorylation/dephosphorylation of Ser404 in the C-terminal domain of tau with wild-type R406 and with the R406W mutation. Ser404 phosphorylation increases the population of *cis*-Pro405 amide bond by stabilizing the *cis*-Pro conformation via a phosphate•••H□-*cis*-Pro C-H/O interaction. The R406W mutation increases the population of *cis*-Pro405 amide bond via an H□-*cis*-Pro-aromatic C-H/□ interaction. Ser404 phosphorylation and R406W substitution individually and in combination significantly stabilize the *cis* amide bond conformation at Pro405. Ser404, with R406 or with the R406W modification, can be phosphorylated by cdk5/p35 and by GSK-3□ at comparable rates. In addition, Ser404 phosphorylation and the R406W substitution increase order in structures with *trans*-Pro. Surprisingly, the R406W mutation makes pSer404 substantially more prone, and pSer409 modestly more prone, to dephosphorylation, within these *tau*<sub>395,411</sub> peptide sequences.

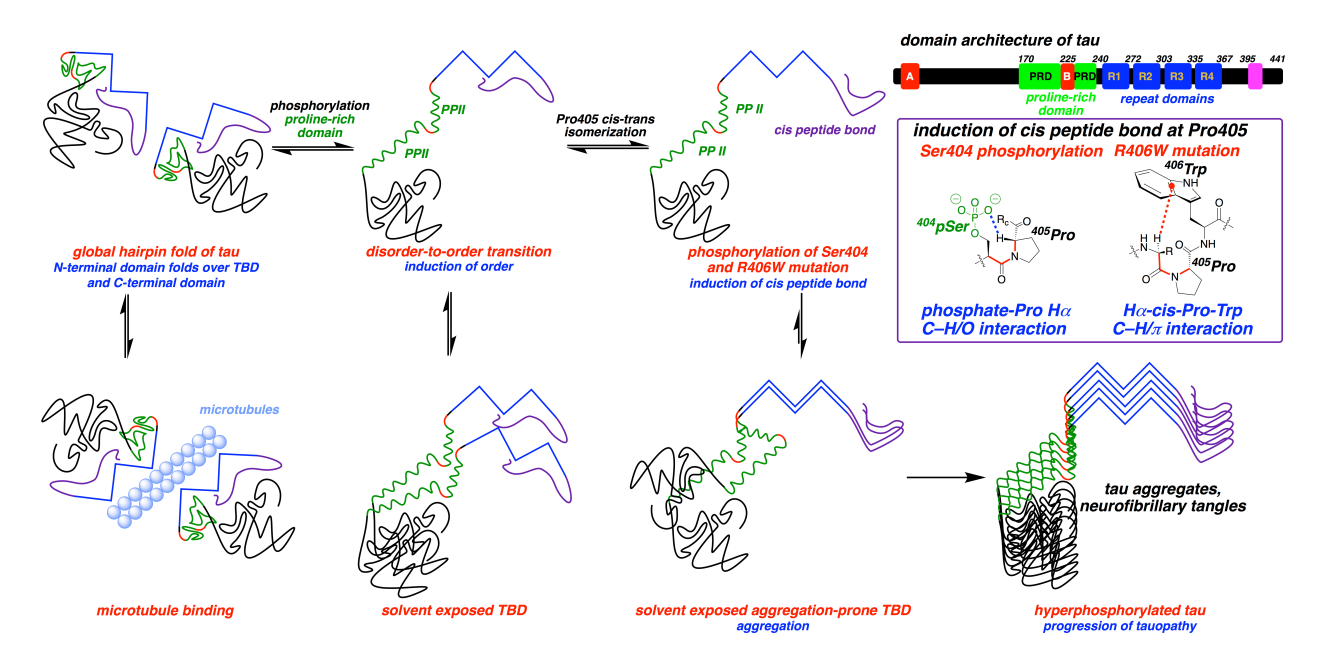


Figure 12. Model of phosphorylation-dependent tau aggregation and conformational changes. Tau adopts a global hairpin fold and binds microtubules, via the tubulin-binding domain (TBD, blue) stabilizing microtubules in neurons.<sup>27</sup> In its native global-hairpin conformation, the Nterminal and the C-terminal domains of tau interact with and protect the aggregation-prone TBD from self-assembly.<sup>173</sup> Phosphorylation of the proline-rich domain (PRD, green) and the Cterminal domain destabilizes the global hairpin fold and promotes self-assembly of tau. 31,174 Phosphorylation of the proline-rich domain induces a more ordered structure, which can destabilize the global hairpin fold, exposing the hydrophobic TBD to solvent, promoting tau selfassembly and aggregation. <sup>24,38,39,42</sup> In the C-terminal domain, phosphorylation of Ser404 stabilizes the cis-proline amide bond conformation (Pro405) via a phosphate --- cis-Pro-H C-H/O interaction. The cis-Pro405 conformation can also be stabilized by the R406W mutation, via either an  $H \square - cis$ -Pro-aromatic or a cis-Pro- $H \square$ -aromatic  $C - H / \square$  interaction. Phosphorylation at Ser404 in combination with the R406W mutation can significantly stabilize the cis-Pro405 amide bond conformation, via dual C-H/O and C-H/\(\sigma\) interactions. In an alternative model consistent with the data, phopshorylation at Ser404 and/or the R406W mutation could lead to increased order and turn conformations in trans-proline, having a similar effect in promoting more aggregation-prone structures. The conformational changes at sequences N-terminal and Cterminal to the TBD, by leading to increased exposure of the hydrophobic TBD, are hypothesized to promote tau aggregation and neurofibrillary tangle formation.

## **Tables**

**Table 1**. Effects of phosphorylation at Ser404, with Arg or Trp (R406W) C-terminal to proline 405, on the *cis-trans* isomerization equilibrium in  $tau_{395\_411}$  peptides.

peptide	K <sub>trans/cis</sub>	[] <i>G</i> kcal mol <sup>−1</sup>	∏∏ <i>G<sup>a</sup></i> kcal mol <sup>-1</sup>	
tau <sub>395-411</sub> S404 R406	7.8 <sup>b</sup>	-1.22		
<i>tau</i> <sub>395–411</sub> pS404 R406	5.1 <sup>c</sup>	-0.96	-0.25	
<i>tau</i> <sub>395–411</sub> S404 R406W	$7.7^{b}$	-1.21		
<i>tau</i> <sub>395–411</sub> pS404 R406W	4.1 <sup>c</sup>	-0.84	-0.37	

<sup>&</sup>quot;  $\square \square G = \square G_{\text{tau}395-411S404, pH=6.5} - \square G_{\text{tau}395-411pS404, pH=7.2}$ , the difference in free energy for the Pro405 cis-trans isomerization equilibrium with Ser404 and with pSer404 in  $tau_{395-411}$ .  $\square G = -\text{RT} \ln K_{\text{trans/cis}}$ .

**Table 2**. Effects of Ser phosphorylation, with Arg or Trp (R406W) C-terminal to proline, on the proline *cis-trans* isomerization in  $tau_{403-406}$  (Ac-TSPX-NH<sub>2</sub>) peptides.

peptide	K <sub>trans/cis</sub>	[] <i>G</i> kcal mol <sup>−1</sup>	∏∏ <i>G<sup>a</sup></i> kcal mol <sup>-1</sup>	
TSPR	$8.5^{b}$	-1.27		
TpSPR	$5.5^c$	-1.01	-0.26	
<b>TSPW</b>	$7.5^{b}$	-1.19		
<b>TpSPW</b>	$3.2^{c}$	-0.69	-0.50	

 $<sup>^</sup>a$   $\square \square G = \square G_{\text{TSPX, pH }4.0} - \square G_{\text{TpSPX, pH }7.2}$ , the difference in free energy for the *cis-trans* isomerization equilibrium with serine and phosphoserine in the sequence Ac-TSPX-NH<sub>2</sub>(X = Arg/Trp).

<sup>&</sup>lt;sup>b</sup> pH 6.5, 298 K.

<sup>&</sup>lt;sup>c</sup> pH 7.2, 298 K.

<sup>&</sup>lt;sup>b</sup> pH 4.0, 298 K. <sup>c</sup> pH 7.2, 298 K.

**Table 3.** Ser or pSer<sup>a</sup> H $\square$  chemical shifts in the *cis*-Pro and *trans*-Pro conformations, with an arginine or a tryptophan at residue X, in the peptide context Ac-TSPX-NH<sub>2</sub>.

nontido	V	□□ <i>G</i> ,	trans-Pro	<i>cis</i> -Pro	∏∏ser,	<i>trans</i> -Pro	<i>cis</i> -Pro	∏Pro,
pepude	<b>∧</b> trans/cis	kcal mol $^{-1_b}$	SerH∏, ppm	SerH <b>□</b> , ppm	$ppm^c$	ProH <b>□</b> , ppm	ProH <b>□</b> , ppm	$ppm^c$
TSPR	$8.5^{d}$	-0.26	4.79	4.59	-0.20	4.45	~ 4.7 <sup>f</sup>	-0.2
TpSPR	$5.5^e$		4.81	4.68	-0.13	4.44	4.89	-0.45
<b>TSPW</b>	$7.5^{d}$	-0.50	4.74	4.35	-0.39	4.33	4.69	-0.36
<b>TpSPW</b>	$3.2^{e}$		4.69	4.30	-0.39	4.31	~ 4.7 <sup>f</sup>	-0.4

<sup>&</sup>lt;sup>a</sup> Ser/S = serine, pSer/pS = phosphoserine.

 $<sup>^{</sup>b}\Box\Box G = \Box G_{\text{TSPX, pH 4.0}} - \Box G_{\text{TpSPX, pH 7.2}}$ , the difference between the free energies for the *cis-trans* isomerization equilibria of Ser-Pro and pSer-Pro in Ac-TSPX-NH<sub>2</sub>.

 $<sup>^</sup>c \square \square_{Ser} = \square H \square_{trans-Ser/pSer} - \square H \square_{cis-Ser/pSer}$ , the difference between the chemical shifts of Ser or pSer H $\square$  in the trans-Pro and cis-Pro conformations.  $\square \square_{Pro} = \square H \square_{trans-Pro} - \square H \square_{cis-Pro}$ , the difference between the chemical shifts of Pro H $\square$  in the trans-Pro and cis-Pro conformations.

<sup>&</sup>lt;sup>d</sup> pH 4.0, 298 K.

<sup>&</sup>lt;sup>e</sup> pH 7.2, 298 K.

<sup>&</sup>lt;sup>f</sup> This resonance overlaps with the resonance for  $H_2O$ , precluding precise determination of  $\square$ .

## References

- (1) Iqbal, K.; Liu, F.; Gong, C. X. Tau and neurodegenerative disease: the story so far. *Nat. Rev. Neurology* **2016**, *12*, 10.1038/nrneurol.2015.1225.
- (2) Nizynski, B.; Dzwolak, W.; Nieznanski, K. Amyloidogenesis of Tau protein. *Protein Sci.* **2017**, *26*, 2126-2150.
- (3) Avila, J.; Jimenez, J. S.; Sayas, C. L.; Bolos, M.; Zabala, J. C.; Rivas, G.; Hernandez, F. Tau Structures. *Front. Aging Neurosci.* **2016**, *8*, 10.3389/fnagi.2016.00262.
- (4) Arendt, T.; Stieler, J. T.; Holzer, M. Tau and tauopathies. *Brain Res. Bull.* **2016**, *126*, 238-292.
- (5) Wang, Y. P.; Mandelkow, E. Tau in physiology and pathology. *Nat. Rev. Neurosci.* **2016**, *17*, 5-21.
- (6) Kumar, H.; Udgaonkar, J. B. Mechanistic approaches to understand the prion-like propagation of aggregates of the human tau protein. *BBA-Proteins Proteom.* **2019**, *1867*, 922-932.
- (7) Chu, D. D.; Liu, F. Pathological Changes of Tau Related to Alzheimer's Disease. *ACS Chem. Neurosci.* **2019**, *10*, 931-944.
- (8) Sanders, D. W.; Kaufman, S. K.; DeVos, S. L.; Sharma, A. M.; Mirbaha, H.; Li, A. M.; Barker, S. J.; Foley, A. C.; Thorpe, J. R.; Serpell, L. C.; Miller, T. M.; Grinberg, L. T.; Seeley, W. W.; Diamond, M. I. Distinct Tau Prion Strains Propagate in Cells and Mice and Define Different Tauopathies. *Neuron* **2014**, *82*, 1271-1288.
- (9) Bibow, S.; Mukrasch, M. D.; Chinnathambi, S.; Biernat, J.; Griesinger, C.; Mandelkow, E.; Zweckstetter, M. The Dynamic Structure of Filamentous Tau. *Angew. Chem., Int. Ed.* **2011**, *50*, 11520-11524.
- (10) Sabbagh, J. J.; Dickey, C. A. The Metamorphic Nature of the Tau Protein: Dynamic Flexibility Comes at a Cost. *Front. Neurosci.* **2016**, *10*, 10.3389/fnins.2016.00003.
- (11) Arakhamia, T.; Lee, C. E.; Carlomagno, Y.; Duong, D. M.; Kundinger, S. R.; Wang, K.; Williams, D.; DeTure, M.; Dickson, D. W.; Cook, C. N.; Seyfried, N. T.; Petrucelli, L.; Fitzpatrick, A. W. P. Posttranslational Modifications Mediate the Structural Diversity of Tauopathy Strains. *Cell* **2020**, *180*, 633-644.
- (12) Wood, J. G.; Mirra, S. S.; Pollock, N. J.; Binder, L. I. Neurofibrillary Tangles of Alzheimer-Disease Share Antigenic Determinants with the Axonal Microtubule-Associated Protein Tau (Tau). *Proc. Natl. Acad. Sci. U.S.A.* **1986**, *83*, 4040-4043.
- (13) Buée, L.; Bussière, T.; Buée-Scherrer, V.; Delacourte, A.; Hof, P. R. Tau protein isoforms, phosphorylation and role in neurodegenerative disorders. *Brain Res. Rev.* **2000**, *33*, 95-130.
- (14) Gong, C. X.; Liu, F.; Grundke-Iqbal, I.; Iqbal, K. Post-translational modifications of tau protein in Alzheimer's disease. *J. Neural Transm.* **2005**, *112*, 813-838.
- (15) Wang, J. Z.; Xia, Y. Y.; Grundke-Iqbal, I.; Iqbal, K. Abnormal Hyperphosphorylation of Tau: Sites, Regulation, and Molecular Mechanism of Neurofibrillary Degeneration. *J. Alzheimers Dis.* **2013**, *33*, S123-S139.
- (16) Zhou, Y.; Shi, J. H.; Chu, D. D.; Hu, W.; Guan, Z. Y.; Gong, C. X.; Iqbal, K.; Liu, F. Relevance of Phosphorylation and Truncation of Tau to the Etiopathogenesis of Alzheimer's Disease. *Front. Aging Neurosci.* **2018**, *10*, 10.3389/fnagi.2018.00027.

- (17) Fitzpatrick, A. W. P.; Falcon, B.; He, S.; Murzin, A. G.; Murshudov, G.; Garringer, H. J.; Crowther, R. A.; Ghetti, B.; Goedert, M.; Scheres, S. H. W. Cryo-EM structures of tau filaments from Alzheimer's disease. *Nature* **2017**, *547*, 185-190.
- (18) Falcon, B.; Zhang, W. J.; Murzin, A. G.; Murshudov, G.; Garringer, H. J.; Vidal, R.; Crowther, R. A.; Ghetti, B.; Scheres, S. H. W.; Goedert, M. Structures of filaments from Pick's disease reveal a novel tau protein fold. *Nature* **2018**, *561*, 137-140.
- (19) Falcon, B.; Zivanov, J.; Zhang, W. J.; Murzin, A. G.; Garringer, H. J.; Vidal, R.; Crowther, R. A.; Newell, K. L.; Ghetti, B.; Goedert, M.; Scheres, S. H. W. Novel tau filament fold in chronic traumatic encephalopathy encloses hydrophobic molecules. *Nature* **2019**, *568*, 420-423.
- (20) Lippens, G.; Gigant, B. Elucidating Tau function and dysfunction in the era of cryo-EM. *J. Biol. Chem.* **2019**, *294*, 9316-9325.
- (21) Steinhilb, M. L.; Dias-Santagata, D.; Mulkearns, E. E.; Shulman, J. M.; Biernat, J.; Mandelkow, E. M.; Feany, M. B. S/P and T/P phosphorylation is critical for tau neurotoxicity in Drosophila. *Journal of Neuroscience Research* **2007**, *85*, 1271-1278.
- (22) Gandhi, N. S.; Landrieu, I.; Byrne, C.; Kukic, P.; Amniai, L.; Cantrelle, F. X.; Wieruszeski, J. M.; Mancera, R. L.; Jacquot, Y.; Lippens, G. A Phosphorylation-Induced Turn Defines the Alzheimer's Disease AT8 Antibody Epitope on the Tau Protein. *Angew. Chem., Int. Ed.* **2015**, *54*, 6819-6823.
- (23) Schwalbe, M.; Kadavath, H.; Biernat, J.; Ozenne, V.; Blackledge, M.; Mandelkow, E.; Zweckstetter, M. Structural Impact of Tau Phosphorylation at Threonine 231. *Structure* **2015**, *23*, 1448-1458.
- (24) Despres, C.; Byrne, C.; Qi, H.; Cantrelle, F. X.; Huvent, I.; Chambraud, B.; Baulieu, E. E.; Jacquot, Y.; Landrieu, I.; Lippens, G.; Smet-Nocca, C. Identification of the Tau phosphorylation pattern that drives its aggregation. *Proc. Natl. Acad. Sci. U.S.A.* **2017**, *114*, 9080-9085.
- (25) McKee, A. C.; Daneshvar, D. H.; Alvarez, V. E.; Stein, T. D. The neuropathology of sport. *Acta Neuropathologica* **2014**, *127*, 29-51.
- (26) McKee, A. C.; Cairns, N. J.; Dickson, D. W.; Folkerth, R. D.; Keene, C. D.; Litvan, I.; Perl, D. P.; Stein, T. D.; Vonsattel, J. P.; Stewart, W.; Tripodis, Y.; Crary, J. F.; Bieniek, K. F.; Dams-O'Connor, K.; Alvarez, V. E.; Gordon, W. A. The first NINDS/NIBIB consensus meeting to define neuropathological criteria for the diagnosis of chronic traumatic encephalopathy. *Acta Neuropathologica* **2016**, *131*, 75-86.
- (27) Jeganathan, S.; von Bergen, M.; Brutlach, H.; Steinhoff, H.-J.; Mandelkow, E. Global hairpin folding of tau in solution. *Biochemistry* **2006**, *45*, 2283-2293.
- (28) Schwalbe, M.; Ozenne, V.; Bibow, S.; Jaremko, M.; Jaremko, L.; Gajda, M.; Jensen, M. R.; Biernat, J.; Becker, S.; Mandelkow, E.; Zweckstetter, M.; Blackledge, M. Predictive Atomic Resolution Descriptions of Intrinsically Disordered hTau40 and alpha-Synuclein in Solution from NMR and Small Angle Scattering. *Structure* **2014**, *22*, 238-249.
- (29) Di Primio, C.; Quercioli, V.; Siano, G.; Rovere, M.; Kovacech, B.; Novak, M.; Cattaneo, A. The Distance between N and C Termini of Tau and of FTDP-17 Mutants Is Modulated by Microtubule Interactions in Living Cells. *Front. Mol. Neurosci.* **2017**, *10*, 10.3389/fnmol.2017.00210.
- (30) Popov, K. I.; Makepeace, K. A. T.; Petrotchenko, E. V.; Dokholyan, N. V.; Borchers, C. H. Insight into the Structure of the "Unstructured" Tau Protein. *Structure* **2019**, *27*, 1710-1715.

- (31) Bibow, S.; Ozenne, V.; Biernat, J.; Blackledge, M.; Mandelkow, E.; Zweckstetter, M. Structural Impact of Proline-Directed Pseudophosphorylation at AT8, AT100, and PHF1 Epitopes on 441-Residue Tau. *J. Am. Chem. Soc.* **2011**, *133*, 15842-15845.
- (32) Combs, B.; Voss, K.; Gamblin, T. C. Pseudohyperphosphorylation Has Differential Effects on Polymerization and Function of Tau Isoforms. *Biochemistry* **2011**, *50*, 9446-9456.
- (33) Chin, A. F.; Toptygin, D.; Elam, W. A.; Schrank, T. P.; Hilser, V. J. Phosphorylation Increases Persistence Length and End-to-End Distance of a Segment of Tau Protein. *Biophys. J.* **2016**, *110*, 362-371.
- (34) Jeganathan, S.; Hascher, A.; Chinnathambi, S.; Biernat, J.; Mandelkow, E. M.; Mandelkow, E. Proline-directed Pseudo-phosphorylation at AT8 and PHF1 Epitopes Induces a Compaction of the Paperclip Folding of Tau and Generates a Pathological (MC-1) Conformation. *J. Biol. Chem.* **2008**, *283*, 32066-32076.
- (35) Kiris, E.; Ventimiglia, D.; Sargin, M. E.; Gaylord, M. R.; Altinok, A.; Rose, K.; Manjunath, B. S.; Jordan, M. A.; Wilson, L.; Feinstein, S. C. Combinatorial Tau Pseudophosphorylation MARKEDLY DIFFERENT REGULATORY EFFECTS ON MICROTUBULE ASSEMBLY AND DYNAMIC INSTABILITY THAN THE SUM OF THE INDIVIDUAL PARTS. *J. Biol. Chem.* **2011**, *286*, 14257-14270.
- (36) Haase, C.; Stieler, J. T.; Arendt, T.; Holzer, M. Pseudophosphorylation of tau protein alters its ability for self-aggregation. *J. Neurochem.* **2004**, *88*, 1509-1520.
- (37) Necula, M.; Kuret, J. Pseudophosphorylation and glycation of tau protein enhance but do not trigger fibrillization in vitro. *J. Biol. Chem.* **2004**, *279*, 49694-49703.
- (38) Bielska, A. A.; Zondlo, N. J. Hyperphosphorylation of tau induces local polyproline II helix. *Biochemistry* **2006**, *45*, 5527-5537.
- (39) Brister, M. A.; Pandey, A. K.; Bielska, A. A.; Zondlo, N. J. OGlcNAcylation and Phosphorylation Have Opposing Structural Effects in tau: Phosphothreonine Induces Particular Conformational Order. *J. Am. Chem. Soc.* **2014**, *136*, 3803-3816.
- (40) Pandey, A. K.; Ganguly, H. K.; Sinha, S. K.; Daniels, K. E.; Yap, G. P. A.; Patel, S.; Zondlo, N. J. An Inherent Structural Difference Between Serine and Threonine Phosphorylation: Phosphothreonine Prefers an Ordered, Compact, Cyclic Conformation. *bioRxiv* **2020**, DOI: 10.1101/2020.1102.1129.971382.
- (41) Amniai, L.; Lippens, G.; Landrieu, I. Characterization of the AT180 epitope of phosphorylated Tau protein by a combined nuclear magnetic resonance and fluorescence spectroscopy approach. *Biochem. Biophys. Res. Comm.* **2011**, *412*, 743-746.
- (42) Sibille, N.; Huvent, I.; Fauquant, C.; Verdegem, D.; Amniai, L.; Leroy, A.; Wieruszeski, J. M.; Lippens, G.; Landrieu, I. Structural characterization by nuclear magnetic resonance of the impact of phosphorylation in the proline-rich region of the disordered Tau protein. *Proteins* **2012**, *80*, 454-462.
- (43) Martin, E. W.; Holehouse, A. S.; Grace, C. R.; Hughes, A.; Pappu, R. V.; Mittag, T. Sequence Determinants of the Conformational Properties of an Intrinsically Disordered Protein Prior to and upon Multisite Phosphorylation. *J. Am. Chem. Soc.* **2016**, *138*, 15323-15335.
- (44) Kumar, A.; Narayanan, V.; Sekhar, A. Characterizing Post-Translational Modifications and Their Effects on Protein Conformation Using NMR Spectroscopy. *Biochemistry* **2020**, *59*, 57-73.
- (45) Schutkowski, M.; Bernhardt, A.; Zhou, X. Z.; Shen, M. H.; Reimer, U.; Rahfeld, J. U.; Lu, K. P.; Fischer, G. Role of phosphorylation in determining the backbone dynamics of

- the serine/threonine-proline motif and Pin1 substrate recognition. *Biochemistry* **1998**, *37*, 5566-5575.
- (46) Lu, P. J.; Wulf, G.; Zhou, X. Z.; Davies, P.; Lu, K. P. The prolyl isomerase Pin1 restores the function of Alzheimer-associated phosphorylated tau protein. *Nature* **1999**, *399*, 784-788.
- (47) Zhou, X. Z.; Kops, O.; Werner, A.; Lu, P. J.; Shen, M. H.; Stoller, G.; Kullertz, G.; Stark, M.; Fischer, G.; Lu, K. P. Pin1-dependent prolyl isomerization regulates dephosphorylation of Cdc25C and tau proteins. *Mol. Cell* **2000**, *6*, 873-883.
- (48) Giustiniani, J.; Guillemeau, K.; Dounane, O.; Sardin, E.; Huvent, I.; Schmitt, A.; Hamdane, M.; Buee, L.; Landrieu, I.; Lippens, G.; Baulieu, E. E.; Chambraud, B. The FK506-binding protein FKBP52 in vitro induces aggregation of truncated Tau forms with prion-like behavior. *FASEB J.* **2015**, *29*, 3171-3181.
- (49) Blair, L. J.; Baker, J. D.; Sabbagh, J. J.; Dickey, C. A. The emerging role of peptidyl-prolyl isomerase chaperones in tau oligomerization, amyloid processing, and Alzheimer's disease. *J. Neurochem.* **2015**, *133*, 1-13.
- (50) Ikura, T.; Ito, N. Peptidyl-prolyl isomerase activity of FK506 binding protein 12 prevents tau peptide from aggregating. *Protein Eng. Design Selection* **2013**, *26*, 539-546.
- (51) Landrieu, I.; Smet-Nocca, C.; Amniai, L.; Louis, J. V.; Wieruszeski, J.-M.; Goris, J.; Janssens, V.; Lippens, G. Molecular Implication of PP2A and Pin1 in the Alzheimer's Disease Specific Hyperphosphorylation of Tau. *PLoS One* **2011**, *6*, e21521.
- (52) Ranganathan, R.; Lu, K. P.; Hunter, T.; Noel, J. P. Structural and functional analysis of the mitotic rotamase Pin1 suggests substrate recognition is phosphorylation dependent. *Cell* **1997**, *89*, 875-886.
- (53) Yaffe, M. B.; Schutkowski, M.; Shen, M. H.; Zhou, X. Z.; Stukenberg, P. T.; Rahfeld, J. U.; Xu, J.; Kuang, J.; Kirschner, M. W.; Fischer, G.; Cantley, L. C.; Lu, K. P. Sequence-specific and phosphorylation-dependent proline isomerization: A potential mitotic regulatory mechanism. *Science* **1997**, *278*, 1957-1960.
- (54) Lippens, G.; Landrieu, I.; Smet, C. Molecular mechanisms of the phosphodependent prolyl cis/trans isomerase Pin1. *FEBS J.* **2007**, *274*, 5211-5222.
- (55) Velazquez, H. A.; Hamelberg, D. Dynamical role of phosphorylation on serine/threonine-proline Pin1 substrates from constant force molecular dynamics simulations. *J. Chem. Phys.* **2015**, *142*, 075102.
- (56) Nakamura, K.; Zhou, X. Z.; Lu, K. P. Cis phosphorylated tau as the earliest detectable pathogenic conformation in Alzheimer disease, offering novel diagnostic and therapeutic strategies. *Prion* **2013**, *7*, 117-120.
- (57) Nakamura, K.; Greenwood, A.; Binder, L.; Bigio, E. H.; Denial, S.; Nicholson, L.; Zhou, X. Z.; Lu, K. P. Proline Isomer-Specific Antibodies Reveal the Early Pathogenic Tau Conformation in Alzheimer's Disease. *Cell* **2012**, *149*, 232-244.
- (58) Kondo, A.; Shahpasand, K.; Mannix, R.; Qiu, J. H.; Moncaster, J.; Chen, C. H.; Yao, Y. D.; Lin, Y. M.; Driver, J. A.; Sun, Y.; Wei, S.; Luo, M. L.; Albayram, O.; Huang, P. Y.; Rotenberg, A.; Ryo, A.; Goldstein, L. E.; Pascual-Leone, A.; McKee, A. C.; Meehan, W.; Zhou, X. Z.; Lu, K. P. Antibody against early driver of neurodegeneration cis P-tau blocks brain injury and tauopathy. *Nature* **2015**, *523*, 431-436.
- (59) Werner-Allen, J. W.; Lee, C. J.; Liu, P.; Nicely, N. I.; Wang, S.; Greenleaf, A. L.; Zhou, P. cis-Proline-mediated Ser(P)(5) Dephosphorylation by the RNA Polymerase II Cterminal Domain Phosphatase Ssu72. *J. Biol. Chem.* **2011**, *286*, 5717-5726.

- (60) Xiang, K. H.; Nagaike, T.; Xiang, S.; Kilic, T.; Beh, M. M.; Manley, J. L.; Tong, L. A. Crystal structure of the human symplekin-Ssu72-CTD phosphopeptide complex. *Nature* **2010**, *467*, 729-733.
- (61) Andreotti, A. H. Native State Proline Isomerization: An Intrinsic Molecular Switch. *Biochemistry* **2003**, *42*, 9515-9524.
- (62) Eckert, B.; Martin, A.; Balbach, J.; Schmid, F. X. Prolyl isomerization as a moleular timer in phage infection. *Nature Struct. Mol. Biol.* **2005**, *12*, 619-623.
- (63) Velazquez, H. A.; Hamelberg, D. Conformational Selection in the Recognition of Phosphorylated Substrates by the Catalytic Domain of Human Pin1. *Biochemistry* **2011**, *50*, 9605-9615.
- (64) Ballatore, C.; Lee, V. M. Y.; Trojanowski, J. Q. Tau-mediated neurodegeneration in Alzheimer's disease and related disorders. *Nat. Rev. Neurosci.* **2007**, *8*, 663-672.
- (65) Gotz, J.; Bodea, L. G.; Goedert, M. ALZHEIMER DISEASE Rodent models for Alzheimer disease. *Nat. Rev. Neurosci.* **2018**, *19*, 583-598.
- (66) Mandelkow, E.; von Bergen, M.; Biernat, J.; Mandelkow, E. M. Structural principles of tau and the paired helical filaments of Alzheimer's disease. *Brain Pathology* **2007**, *17*, 83-90.
- (67) Hong, M.; Zhukareva, V.; Vogelsberg-Ragaglia, V.; Wszolek, Z.; Reed, L.; Miller, B. I.; Geschwind, D. H.; Bird, T. D.; McKeel, D.; Goate, A.; Morris, J. C.; Wilhelmsen, K. C.; Schellenberg, G. D.; Trojanowski, J. Q.; Lee, V. M. Y. Mutation-specific functional impairments in distinct Tau isoforms of hereditary FTDP-17. *Science* **1998**, *282*, 1914-1917.
- (68) Strang, K. H.; Golde, T. E.; Giasson, B. I. MAPT mutations, tauopathy, and mechanisms of neurodegeneration. *Lab. Investig.* **2019**, *99*, 912-928.
- (69) Tatebayashi, Y.; Miyasaka, T.; Chui, D. H.; Akagi, T.; Mishima, K.; Iwasaki, K.; Fujiwara, M.; Tanemura, K.; Murayama, M.; Ishiguro, K.; Planel, E.; Sato, S.; Hashikawa, T.; Takashima, A. Tau filament formation and associative memory deficit in aged mice expressing mutant (R406W) human tau. *Proc. Natl. Acad. Sci. U.S.A.* **2002**, *99*, 13896-13901.
- (70) Zhang, B.; Higuchi, M.; Yoshiyama, Y.; Ishihara, T.; Forman, M. S.; Martinez, D.; Joyce, S.; Trojanowski, J. Q.; Lee, V. M. Y. Retarded axonal transport of R406W mutant tau in transgenic mice with a neurodegenerative tauopathy. *J. Neurosci.* **2004**, *24*, 4657-4667.
- (71) de Calignon, A.; Polydoro, M.; Suarez-Calvet, M.; William, C.; Adamowicz, D. H.; Kopeikina, K. J.; Pitstick, R.; Sahara, N.; Ashe, K. H.; Carlson, G. A.; Spires-Jones, T. L.; Hyman, B. T. Propagation of Tau Pathology in a Model of Early Alzheimer's Disease. *Neuron* **2012**, *73*, 685-697.
- (72) Liu, L.; Drouet, V.; Wu, J. W.; Witter, M. P.; Small, S. A.; Clelland, C.; Duff, K. Trans-Synaptic Spread of Tau Pathology In Vivo. *PLoS One* **2012**, *7*, e31302.
- (73) Barghorn, S.; Zheng-Fischhofer, Q.; Ackmann, M.; Biernat, J.; von Bergen, M.; Mandelkow, E. M.; Mandelkow, E. Structure, microtubule interactions, and paired helical filament aggregation by tau mutants of frontotemporal dementias. *Biochemistry* **2000**, *39*, 11714-11721.
- (74) von Bergen, M.; Barghorn, S.; Li, L.; Marx, A.; Biernat, J.; Mandelkow, E. M.; Mandelkow, E. Mutations of tau protein in frontotemporal dementia promote aggregation of paired helical filaments by enhancing local beta-structure. *J. Biol. Chem.* **2001**, *276*, 48165-48174.

- (75) Barghorn, S.; Davies, P.; Mandelkow, E. Tau paired helical filaments from Alzheimer's disease brain and assembled in vitro are based on beta-structure in the core domain. *Biochemistry* **2004**, *43*, 1694-1703.
- (76) Frost, B.; Ollesch, J.; Wille, H.; Diamond, M. I. Conformational Diversity of Wild-type Tau Fibrils Specified by Templated Conformation Change. *J. Biol. Chem.* **2009**, *284*, 3546-3551.
- (77) Hasegawa, M.; Smith, M. J.; Goedert, M. Tau proteins with FTDP-17 mutations have a reduced ability to promote microtubule assembly. *FEBS Lett.* **1998**, *437*, 207-210.
- (78) Dayanandan, R.; Van Slegtenhorst, M.; Mack, T. G. A.; Ko, L.; Yen, S. H.; Leroy, K.; Brion, J. P.; Anderton, B. H.; Hutton, M.; Lovestone, S. Mutations in tau reduce its microtubule binding properties in intact cells and affect its phosphorylation. *FEBS Lett.* **1999**, 446, 228-232.
- (79) Perez, M.; Lim, F.; Arrasate, M.; Avila, J. The FTDP-17-linked mutation R406W abolishes the interaction of phosphorylated tau with microtubules. *J. Neurochem.* **2000**, *74*, 2583-2589.
- (80) Miyasaka, T.; Morishima-Kawashima, M.; Ravid, R.; Heutink, P.; van Swieten, J. C.; Nagashima, K.; Ihara, Y. Molecular analysis of mutant and wild-type tau deposited in the brain affected by the FTDP-17 R406W mutation. *Am. J. Pathol.* **2001**, *158*, 373-379.
- (81) Krishnamurthy, P. K.; Johnson, G. V. W. Mutant (R406W) human tau is hyperphosphorylated and does not efficiently bind microtubules in a neuronal cortical cell model. *J. Biol. Chem.* **2004**, *279*, 7893-7900.
- (82) Ikeda, M.; Shoji, M.; Kawarai, T.; Kawarabayashi, T.; Matsubara, E.; Murakami, T.; Sasaki, A.; Tomidokoro, Y.; Ikarashi, Y.; Kuribara, H.; Ishiguro, K.; Hasegawa, M.; Yen, S. H.; Chishti, M. A.; Harigaya, Y.; Abe, K.; Okamoto, K.; George-Hyslop, P. S.; Westaway, D. Accumulation of filamentous tau in the cerebral cortex of human tau R406W transgenic mice. *Am. J. Pathol.* **2005**, *166*, 521-531.
- (83) Otvos, L.; Feiner, L.; Lang, E.; Szendrei, G. I.; Goedert, M.; Lee, V. M. Y. Monoclonal-Antibody PHF-1 Recognizes Tau-Protein Phosphorylated at Serine Residue-396 and Residue-404. *J. Neurosci. Res.* **1994**, *39*, 669-673.
- (84) Augustinack, J. C.; Schneider, A.; Mandelkow, E. M.; Hyman, B. T. Specific tau phosphorylation sites correlate with severity of neuronal cytopathology in Alzheimer's disease. *Acta Neuropathologica* **2002**, *103*, 26-35.
- (85) Sun, Q.; Gamblin, T. C. Pseudohyperphosphorylation Causing AD-like Changes in Tau Has Significant Effects on Its Polymerization. *Biochemistry* **2009**, *48*, 6002-6011.
- (86) Hanger, D. P.; Hughes, K.; Woodgett, J. R.; Brion, J. P.; Anderton, B. H. Glycogen-Synthase Kinase-3 Induces Alzheimers Disease-Like Phosphorylation of Tau Generation of Paired Helical Filament Epitopes and Neuronal Localization of the Kinase. *Neuroscience Lett.* **1992**, *147*, 58-62.
- (87) Liu, F.; Iqbal, K.; Grundke-Iqbal, I.; Gong, C. X. Involvement of aberrant glycosylation in phosphorylation of tau by cdk5 and GSK-3 beta. *FEBS Lett.* **2002**, *530*, 209-214.
- (88) Liu, S. J.; Zhang, J. Y.; Li, H. L.; Fang, Z. Y.; Wang, Q.; Deng, H. M.; Gong, C. X.; Grundke-Iqbal, I.; Iqbal, K.; Wang, J. Z. Tau becomes a more favorable substrate for GSK-3 when it is prephosphorylated by PKA in rat brain. *J. Biol. Chem.* **2004**, *279*, 50078-50088.

- (89) Liu, F.; Liang, Z. H.; Shi, J. H.; Yin, D. M.; El-Akkad, E.; Grundke-Iqbal, I.; Iqbal, K.; Gong, C. X. PKA modulates GSK-3 beta- and cdk5-catalyzed phosphorylation of tau in site- and kinase-specific manners. *FEBS Lett.* **2006**, *580*, 6269-6274.
- (90) Sengupta, A.; Novak, M.; Grundke-Iqbal, I.; Iqbal, K. Regulation of phosphorylation of tau by cyclin-dependent kinase 5 and glycogen synthase kinase-3 at substrate level. *FEBS Lett.* **2006**, *580*, 5925-5933.
- (91) Wang, J. Z.; Grundke-Iqbal, I.; Iqbal, K. Kinases and phosphatases and tau sites involved in Alzheimer neurofibrillary degeneration. *Eur. J. Neurosci.* **2007**, *25*, 59-68.
- (92) Dyson, H. J.; Rance, M.; Houghten, R. A.; Lerner, R. A.; Wright, P. E. Folding of Immunogenic Peptide-Fragments of Proteins in Water Solution .1. Sequence Requirements for the Formation of a Reverse Turn. *J. Mol. Biol.* **1988**, *201*, 161-200.
- (93) Yao, J.; Dyson, H. J.; Wright, P. E. 3-Dimensional Structure of a Type-VI turn in a Linear Peptide in Water Solution Evidence for Stacking of Aromatic Rings as a Major Stabilizing Factor. *J. Mol. Biol.* **1994**, *243*, 754-766.
- (94) Nardi, F.; Kemmink, J.; Sattler, M.; Wade, R. C. The cisproline(i-1)-aromatic(i) interaction: Folding of the Ala-cisPro-Tyr peptide characterized by NMR and theoretical approaches. *J. Biomol. NMR* **2000**, *17*, 63-77.
- (95) Meng, H. Y.; Thomas, K. M.; Lee, A. E.; Zondlo, N. J. Effects of i and i+3 Residue Identity on Cis-Trans Isomerism of the Aromatic $_{i+1}$ -Prolyl $_{i+2}$  Amide Bond: Implications for Type VI b-turn Formation. *Biopolymers (Peptide Sci.)* **2006**, *84*, 192-204.
- (96) Zondlo, N. J. Aromatic-Proline Interactions: Electronically Tunable CH/pi Interactions. *Acc. Chem. Res.* **2013**, *46*, 1039-1049.
- (97) Ganguly, H. K.; Majumder, B.; Chattopadhyay, S.; Chakrabarti, P.; Basu, G. Direct Evidence for CH...pi Interaction Mediated Stabilization of Pro-cisPro Bond in Peptides with Pro-Pro-Aromatic Motifs. *J. Am. Chem. Soc.* **2012**, *134*, 4661-4669.
- (98) Ganguly, H. K.; Kaur, H.; Basu, G. Local Control of cis-Peptidyl–Prolyl Bonds Mediated by  $CH\cdots\pi$  Interactions: The Xaa-Pro-Tyr Motif. *Biochemistry* **2013**, *52*, 6348-6357.
- (99) Ganguly, H. K.; Elbaum, M. B.; Zondlo, N. J. Proline-Aromatic Sequences Stabilize Turns via  $C-H/\pi$  interactions in both cis-Proline and trans-Proline. *ChemRxiv* **2023**, DOI: 10.26434/chemrxiv-22023-26437nb26444.
- (100) Gong, C. X.; Singh, T. J.; Grundkeiqbal, I.; Iqbal, K. Phosphoprotein Phosphatase-Activities in Alzheimer-Disease Brain. *J. Neurochem.* **1993**, *61*, 921-927.
- (101) Gong, C. X.; Lidsky, T.; Wegiel, J.; Zuck, L.; Grundke-Iqbal, I.; Iqbal, K. Phosphorylation of microtubule-associated protein tau is regulated by protein phosphatase 2A in mammalian brain Implications for neurofibrillary degeneration in Alzheimer's disease. *J. Biol. Chem.* **2000**, *275*, 5535-5544.
- (102) Liu, F.; Grundke-Iqbal, I.; Iqbal, K.; Gong, C. X. Contributions of protein phosphatases PP1, PP2A, PP2B and PP5 to the regulation of tau phosphorylation. *European Journal of Neuroscience* **2005**, *22*, 1942-1950.
- (103) Qian, W.; Shi, J. H.; Yin, X. M.; Iqbal, K.; Grundke-Iqbal, I.; Gong, C. X.; Liu, F. PP2A Regulates Tau Phosphorylation Directly and also Indirectly via Activating GSK-3 beta. *J. Alzheimers Dis.* **2010**, *19*, 1221-1229.
- (104) Dajani, R.; Fraser, E.; Roe, S. M.; Young, N.; Good, V.; Dale, T. C.; Pearl, L. H. Crystal Structure of Glycogen Synthase Kinase-3b: Structural Basis for Phosphate-Primed Substrate Specificity and Autoinhibition. *Cell* **2001**, *105*, 721-732.

- (105) Ganguly, H. K.; Basu, G. CH center dot center dot center dot pi interaction mediated stabilization of cisPro bond: New sequence motifs. *Biopolymers* **2011**, *96*, 430-430.
- (106) Vuister, G. W.; Bax, A. Quantitative J Correlation: A New Approach for Measuring Homonuclear Three-Bond  $J_{\rm HNHa}$  Coupling Constants in <sup>15</sup>N-enriched Proteins. J. Am. Chem. Soc. **1993**, 115, 7772-7777.
- (107) Brown, A. M.; Zondlo, N. J. A Propensity Scale for Type II Polyproline Helices (PPII): Aromatic Amino Acids in Proline-Rich Sequences Strongly Disfavor PPII Due to Proline-Aromatic Interactions. *Biochemistry* **2012**, *51*, 5041-5051.
- (108) Elbaum, M. B.; Zondlo, N. J. OGlcNAcylation and Phosphorylation Have Similar Structural Effects in  $\alpha$ -Helices: Post-Translational Modifications as Inducible Start and Stop Signals in  $\alpha$ -Helices, with Greater Structural Effects on Threonine Modification. *Biochemistry* **2014**, *53*, 2242-2260.
- (109) Tholey, A.; Lindemann, A.; Kinzel, V.; Reed, J. Direct effects of phosphorylation on the preferred backbone conformation of peptides: A nuclear magnetic resonance study. *Biophysical J.* **1999**, *76*, 76-87.
- (110) Conibear, A. C.; Rosengren, K. J.; Becker, C. F. W.; Kaehlig, H. Random coil shifts of posttranslationally modified amino acids. *J. Biomol. NMR* **2019**, *73*, 587-599.
- (111) Hendus-Altenburger, R.; Fernandes, C. B.; Bugge, K.; Kunze, M. B. A.; Boomsma, W.; Kragelund, B. B. Random coil chemical shifts for serine, threonine and tyrosine phosphorylation over a broad pH range. *J. Biomol. NMR* **2019**, *73*, 713-725.
- (112) Kemp, B. E.; Pearson, R. B. Design and Use of Peptide-Substrates for Protein-Kinases. *Methods Enzymol.* **1991**, *200*, 121-134.
- (113) Songyang, Z.; Blechner, S.; Hoagland, N.; Hoekstra, M. F.; Piwnica-Worms, H.; Cantley, L. C. Use of an Oriented Peptide Library to Determine the Optimal Substrates of Protein-Kinases. *Curr. Biol.* **1994**, *4*, 973-982.
- (114) Hutti, J. E.; Jarrell, E. T.; Chang, J. D.; Abbott, D. W.; Storz, P.; Toker, A.; Cantley, L. C.; Turk, B. E. A rapid method for determining protein kinase phosphorylation specificity. *Nat. Methods* **2004**, *1*, 27-29.
- (115) Baumann, K.; Mandelkow, E. M.; Biernat, J.; Piwnicaworms, H.; Mandelkow, E. Abnormal Alzheimer-Like Phosphorylation of Tau-Protein by Cyclin-Dependent Kinases Cdk2 and Cdk5. *FEBS Lett.* **1993**, *336*, 417-424.
- (116) Trinczek, B.; Biernat, J.; Baumann, K.; Mandelkow, E. M.; Mandelkow, E. Domains of Tau-Protein, Differential Phosphorylation, and Dynamic Instability of Microtubules. *Mol. Biol. Cell* **1995**, *6*, 1887-1902.
- (117) Mok, J.; Kim, P. M.; Lam, H. Y. K.; Piccirillo, S.; Zhou, X. Q.; Jeschke, G. R.; Sheridan, D. L.; Parker, S. A.; Desai, V.; Jwa, M.; Cameroni, E.; Niu, H. Y.; Good, M.; Remenyi, A.; Ma, J. L. N.; Sheu, Y. J.; Sassi, H. E.; Sopko, R.; Chan, C. S. M.; De Virgilio, C.; Hollingsworth, N. M.; Lim, W. A.; Stern, D. F.; Stillman, B.; Andrews, B. J.; Gerstein, M. B.; Snyder, M.; Turk, B. E. Deciphering Protein Kinase Specificity Through Large-Scale Analysis of Yeast Phosphorylation Site Motifs. *Sci. Signal.* **2010**, *3*, ra12.
- (118) Planel, E.; Yasutake, K.; Fujita, S. C.; Ishiguro, K. Inhibition of protein phosphatase 2A overrides tau protein kinase I/glycogen synthase kinase 3 beta and cyclin-dependent kinase 5 inhibition and results in tau hyperphosphorylation in the hippocampus of starved mouse. *J. Biol. Chem.* **2001**, *276*, 34298-34306.

- (119) Martin, L.; Latypova, X.; Wilson, C. M.; Magnaudeix, A.; Perrin, M. L.; Terro, F. Tau protein phosphatases in Alzheimer's disease: The leading role of PP2A. *Ageing Res. Rev.* **2013**, *12*, 39-49.
- (120) Burkholder, N. T.; Medellin, B.; Irani, S.; Matthews, W.; Showalter, S. A.; Zhang, Y. J. Chemical Tools for Studying the Impact of cis/trans Prolyl Isomerization on Signaling: A Case Study on RNA Polymerase II Phosphatase Activity and Specificity. *Meth. Enzymol.* **2018**, *607*, 269-297.
- (121) Stewart, D. E.; Sarkar, A.; Wampler, J. E. Occurrence and role of cis peptidebonds in protein structures. *J. Mol. Biol.* **1990**, *214*, 253-260.
- (122) Pal, D.; Chakrabarti, P. Cis Peptide Bonds in Proteins: Residues Involved, their Conformations, Interactions and Locations. *J. Mol. Biol.* **1999**, *294*, 271-288.
- (123) MacArthur, M. W.; Thornton, J. M. Influence of proline residues on protein conformation. *J. Mol. Biol.* **1991**, *218*, 397-412.
- (124) Krimm, S. Hydrogen Bonding of C-H...O=C in Proteins. Science 1967, 158, 530-531.
- (125) Derewenda, Z. S.; Lee, L.; Derewenda, U. The Occurence of C–H...O Hydrogen Bonds in Proteins. *J. Mol. Biol.* **1995**, *252*, 248-262.
- (126) Desiraju, G. R. The C–H...O Hydrogen Bond: Structural Implications and Supramolecular Design. *Acc. Chem. Res.* **1996**, *29*, 441-449.
- (127) Gu, Y. L.; Kar, T.; Scheiner, S. Fundamental properties of the CH center dot center dot center dot O interaction: Is it a true hydrogen bond? *J. Am. Chem. Soc.* **1999**, *121*, 9411-9422.
- (128) Shi, Z. S.; Olson, C. A.; Bell, A. J.; Kallenbach, N. R. Stabilization of alpha-helix structure by polar side-chain interactions: Complex salt bridges, cation-pi interactions, and C-H center dot center dot O H-bonds. *Biopolymers* **2001**, *60*, 366-380.
- (129) Castellano, R. K. Progress toward understanding the nature and function of C-H center dot center dot center dot O interactions. *Curr. Org. Chem.* **2004**, *8*, 845-865.
- (130) Manikandan, K.; Ramakumar, S. The occurrence of C-H center dot center dot center dot O hydrogen bonds in alpha-helices and helix termini in globular proteins. *Proteins* **2004**, *56*, 768-781.
- (131) Horowitz, S.; Trievel, R. C. Carbon-Oxygen Hydrogen Bonding in Biological Structure and Function. *J. Biol. Chem.* **2012**, *287*, 41576-41582.
- (132) Jones, C. R.; Baruah, P. K.; Thompson, A. L.; Scheiner, S.; Smith, M. D. Can a C-H center dot center dot Confermation? *J. Am. Chem. Soc.* **2012**, *134*, 12064-12071.
- (133) Driver, R. W.; Claridge, T. D. W.; Scheiner, S.; Smith, M. D. Torsional and Electronic Factors Control the C-H center dot center dot O Interaction. *Chem. Eur. J.* **2016**, *22*, 16513-16521.
- (134) Daniecki, N. J.; Bhatt, M. R.; Yap, G. P. A.; Zondlo, N. J. Proline C-H Bonds as Loci for Proline Assembly via C-H/O Interactions. *ChemBioChem* **2022**, *23*, e202200409.
- (135) Nepal, B.; Scheiner, S. Anionic CH center dot center dot center dot X- Hydrogen Bonds: Origin of Their Strength, Geometry, and Other Properties. *Chem. Eur. J.* **2015**, *21*, 1474-1481.
- (136) Frisch, M. J.; Trucks, G. W.; Schlegel, H. B.; Scuseria, G. E.; Robb, M. A.; Cheeseman, J. R.; Scalmani, G.; Barone, V.; Mennucci, B.; Petersson, G. A.; Nakatsuji, H.; Caricato, M.; Li, X.; Hratchian, H. P.; Izmaylov, A. F.; Bloino, J.; Zheng, G.; Sonnenberg, J. L.;

- Hada, M.; Ehara, M.; Toyota, K.; Fukuda, R.; Hasegawa, J.; Ishida, M.; Nakajima, T.; Honda, Y.; Kitao, O.; Nakai, H.; Vreven, T.; Montgomery, J., J. A.; Peralta, J. E.; Ogliaro, F.; Bearpark, M.; Heyd, J. J.; Brothers, E.; Kudin, K. N.; Staroverov, V. N.; Keith, T.; Kobayashi, R.; Normand, J.; Raghavachari, K.; Rendell, A.; Burant, J. C.; Iyengar, S. S.; Tomasi, J.; Cossi, M.; Rega, N.; Millam, J. M.; Klene, M.; Knox, J. E.; Cross, J. B.; Bakken, V.; Adamo, C.; Jaramillo, J.; Gomperts, R.; Stratmann, R. E.; Yazyev, O.; Austin, A. J.; Cammi, R.; Pomelli, C.; Ochterski, J. W.; Martin, R. L.; Morokuma, K.; Zakrzewski, V. G.; Voth, G. A.; Salvador, P.; Dannenberg, J. J.; Dapprich, S.; Daniels, A. D.; Farkas, O.; Foresman, J. B.; Ortiz, J. V.; Cioslowski, J.; Fox, D. J.: Gaussian 09, Revision D.01. Gaussian, Inc.: Wallingford, CT, 2013.
- (137) Dunning, T. H., Jr. Gaussian basis sets for use in correlated molecular calculations: The atoms boron through neon and hydrogen. *J. Chem. Phys.* **1989**, *90*, 1007-1023.
- (138) Raghavachari, K.; Binkley, J. S.; Seeger, R.; Pople, J. A. Self-Consistent Molecular Orbital Methods. 20. Basis sets for correlated wave functions. *J. Chem. Phys.* **1980**, 72, 650-654.
- (139) Frisch, M. J.; Head-Gordon, M.; Pople, J. A. Direct MP2 gradient method. *Chem. Phys. Lett.* **1990**, *166*, 275-280.
- (140) Zhao, Y.; Truhlar, D. G. The M06 suite of density functionals for main group thermochemistry, thermochemical kinetics, noncovalent interactions, excited states, and transition elements: two new functionals and systematic testing of four M06-class functionals and 12 other functionals. *Theor. Chem. Acc.* **2008**, *120*, 215-241.
- (141) Reed, A. E.; Curtiss, L. A.; Weinhold, F. Intermolecular Interactions from a Natural Bond Orbital, Donor-Acceptor Viewpoint. *Chem. Rev.* **1988**, *88*, 899-926.
- (142) Glendening, C. R.; Landis, C. R.; Weinhold, F. Natural bond orbital methods. *WIREs Comput. Mol. Sci.* **2012**, *2*, 1-42.
- (143) Lodge, J. A.; Maier, T.; Liebl, W.; Hoffmann, V.; Strater, N. Crystal structure of Thermotoga maritima alpha-glucosidase AglA defines a new clan of NAD(+)-dependent glycosidases. *J. Biol. Chem.* **2003**, *278*, 19151-19158.
- (144) Pavone, V.; Gaeta, G.; Lombardi, A.; Nastri, F.; Maglio, O.; Isernia, C.; Saviano, M. Discovering Protein Secondary Structures: Classification and Description of Isolated alpha-Turns. *Biopolymers* **1996**, *38*, 705-721.
- (145) Chou, K. C. Prediction and classification of  $\alpha$ -turn types. *Biopolymers* **1997**, *42*, 837-853.
- (146) Wilmot, C. M.; Thornton, J. M. Analysis and Prediction of the Different Types of Beta-Turn in Proteins. *J. Mol. Biol.* **1988**, *203*, 221-232.
- (147) Hutchinson, E. G.; Thornton, J. M. A revised set of potentials for beta-turn formation in proteins. *Protein Sci.* **1994**, *3*, 2207-2216.
- (148) Yao, J.; Feher, V. A.; Espejo, B. F.; Reymond, M. T.; Wright, P. E.; Dyson, H. J. Stabilization of a Type-VI Turn in a Family of Linear Peptides in Water Solution. *J. Mol. Biol.* **1994**, *243*, 736-753.
- (149) Dasgupta, R.; Ganguly, H. K.; Modugula, E. K.; Basu, G. Type VIa beta-turn-fused helix N-termini: A novel helix N-cap motif containing cis proline. *Peptide Sci.* **2017**, *108*, e22919.
- (150) Shapovalov, M.; Vucetic, S.; Dunbrack, R. L., Jr. A new clustering and nomenclature for beta turns derived from high-resolution protein structures. *PLoS Comput. Biol.* **2019**, *15*, e1006844.

- (151) Smet, C.; Leroy, A.; Sillen, A.; Wieruszeski, J.-M.; Landrieu, I.; Lippens, G. Accepting its random coil nature allows a partial NMR assignment of the neuronal tau protein. *ChemBioChem* **2004**, *5*, 1639-1646.
- (152) Mukrasch, M. D.; Bibow, S.; Korukottu, J.; Jeganathan, S.; Biernat, J.; Griesinger, C.; Mandelkow, E.; Zweckstetter, M. Structural Polymorphism of 441-Residue Tau at Single Residue Resolution. *PloS Biology* **2009**, *7*, 399-414.
- (153) Mandelkow, E. M.; Drewes, G.; Biernat, J.; Gustke, N.; Vanlint, J.; Vandenheede, J. R.; Mandelkow, E. Glycogen-Synthase Kinase-3 and the Alzheimer-Like State of Microtubule-Associated Protein Tau. *FEBS Lett.* **1992**, *314*, 315-321.
- (154) Brandts, J. F.; Halvorson, H. R.; Brennan, M. Consideration of Possibility That Slow Step in Protein Denaturation Reactions Is Due to Cis-Trans Isomerism of Proline Residues. *Biochemistry* **1975**, *14*, 4953-4963.
- (155) Wedemeyer, W. J.; Welker, E.; Scheraga, H. A. Proline cis-trans isomerization and protein folding. *Biochemistry* **2002**, *41*, 14637-14644.
- (156) Schmidpeter, P. A. M.; Koch, J. R.; Schmid, F. X. Control of protein function by prolyl isomerization. *Biochim. Biophys. Acta Gen. Subj.* **2015**, *1850*, 1973-1982.
- (157) Yotsumoto, K.; Saito, T.; Asada, A.; Oikawa, T.; Kimura, T.; Uchida, C.; Ishiguro, K.; Uchida, T.; Hasegawa, M.; Hisanaga, S. Effect of Pin1 or Microtubule Binding on Dephosphorylation of FTDP-17 Mutant Tau. *J. Biol. Chem.* **2009**, *284*, 16840-16847.
- (158) Reimer, U.; Scherer, G.; Drewello, M.; Kruber, S.; Schutkowski, M.; Fischer, G. Side-chain effects on peptidyl-prolyl cis/trans isomerization. *J. Mol. Biol.* **1998**, *279*, 449-460.
- (159) Montelione, G. T.; Arnold, E.; Meinwald, Y. C.; Stimson, E. R.; Denton, J. B.; Huang, S. G.; Clardy, J.; Scheraga, H. A. Chain-Folding Initiation Structures in Ribonuclease-a Conformational-Analysis of Trans-Ac-Asn-Pro-Tyr-NHMe and Trans-Ac-Tyr-Pro-Asn-NHMe in Water and in the Solid-State. *J. Am. Chem. Soc.* **1984**, *106*, 7946-7958.
- (160) Liou, Y. C.; Sun, A.; Ryo, A.; Zhou, X. Z.; Yu, Z. X.; Huang, H. K.; Uchida, T.; Bronson, R.; Bing, G. Y.; Li, X. J.; Hunter, T.; Lu, K. P. Role of the prolyl isomerase Pin1 in protecting against age-dependent neurodegeneration. *Nature* **2003**, *424*, 556-561.
- (161) Luo, Y. H.; Yogesha, S. D.; Cannon, J. R.; Yan, W. P.; Ellington, A. D.; Brodbelt, J. S.; Zhang, Y. Novel Modifications on C-terminal Domain of RNA Polymerase II Can Finetune the Phosphatase Activity of Ssu72. *ACS Chem. Biol.* **2013**, *8*, 2042-2052.
- (162) Bataille, A. R.; Jeronimo, C.; Jacques, P. E.; Laramee, L.; Fortin, M. E.; Forest, A.; Bergeron, M.; Hanes, S. D.; Robert, F. A Universal RNA Polymerase II CTD Cycle Is Orchestrated by Complex Interplays between Kinase, Phosphatase, and Isomerase Enzymes along Genes. *Mol. Cell* **2012**, *45*, 158-170.
- (163) Corden, J. L. RNA Polymerase II C-Terminal Domain: Tethering Transcription to Transcript and Template. *Chem. Rev.* **2013**, *113*, 8423-8455.
- (164) Eick, D.; Geyer, M. The RNA Polymerase II Carboxy-Terminal Domain (CTD) Code. *Chem. Rev.* **2013**, *113*, 8456-8490.
- (165) Jeronimo, C.; Bataille, A. R.; Robert, F. The Writers, Readers, and Functions of the RNA Polymerase II C-Terminal Domain Code. *Chem. Rev.* **2013**, *113*, 8491-8522.
- (166) Zhou, X. Z.; Lu, K. P. The isomerase PIN1 controls numerous cancer-driving pathways and is a unique drug target. *Nature Reviews Cancer* **2016**, *16*, 463-478.
- (167) Walker, L. C.; Diamond, M. I.; Duff, K. E.; Hyman, B. T. Mechanisms of Protein Seeding in Neurodegenerative Diseases. *Jama Neurology* **2013**, *70*, 304-310.

- (168) Mirbaha, H.; Holmes, B. B.; Sanders, D. W.; Bieschke, J.; Diamond, M. I. Tau Trimers Are the Minimal Propagation Unit Spontaneously Internalized to Seed Intracellular Aggregation. *J. Biol. Chem.* **2015**, *290*, 14893-14903.
- (169) Kaufman, S. K.; Sanders, D. W.; Thomas, T. L.; Ruchinskas, A. J.; Vaquer-Alicea, J.; Sharma, A. M.; Miller, T. M.; Diamond, M. I. Tau Prion Strains Dictate Patterns of Cell Pathology, Progression Rate, and Regional Vulnerability In Vivo. *Neuron* **2016**, *92*, 796-812.
- (170) Wang, G.; Dunbrack, R. L. PISCES: a protein sequence culling server. *Bioinformatics* **2003**, *19*, 1589-1591.
- (171) Fushinobu, S.; Saku, T.; Hidaka, M.; Jun, S.-Y.; Nojiri, H.; Yamane, H.; Shoun, H.; Omori, T.; Wakagi, T. Crystal structures of a meta-cleavage product hydrolase from Pseudomonas fluorescens IP01 (CumD) complexed with cleavage products. *Protein Sci.* **2002**, *11*, 2184-2195.
- (172) Wright, C. S.; Mi, L. Z.; Lee, S.; Rastinejad, F. Crystal Structure Analysis of Phosphatidylcholine-GM2-Activator Product Complexes: Evidence for Hydrolase Activity. *Biochemistry* **2005**, *44*, 13510-13521.
- (173) Kolarova, M.; García-Sierra, F.; Bartos, A.; Ricny, J.; Ripova, D. Structure and pathology of tau protein in Alzheimer disease. *Int. J. Alzheimers Dis.* **2012**, 2012, article ID 731526.
- (174) Alonso, A. D.; Zaidi, T.; Novak, M.; Grundke-Iqbal, I.; Iqbal, K. Hyperphosphorylation induces self-assembly of tau into tangles of paired helical filaments/straight filaments. *Proc. Natl. Acad. Sci. U.S.A.* **2001**, *98*, 6923-6928.

## **Graphical Table of Contents**

